STABILITY OF NANO-ENGINEERED C_{60} COLLOIDAL SUSPENSIONS IN WATER AND ITS OXIDATIVE BEHAVIOR

By

BEFRIKA S. MURDIANTI

Bachelor of Science in Chemistry
Institut Teknologi Bandung
Bandung, West Java, INDONESIA
2000

Master of Science in Chemistry
The University of Tulsa
Tulsa, OK
2007

Submitted to the Faculty of the
Graduate College of the
Oklahoma State University
in partial fulfillment of
the requirements for
the Degree of
DOCTOR OF PHILOSOPHY
July, 2012

STABILITY OF NANO-ENGINEERED C_{60}

COLLOIDAL SUSPENSIONS IN WATER AND ITS

OXIDATIVE BEHAVIOR

Dissertation Approved:

Dr. Kevin Ausman

Dissertation Adviser

Dr. Frank Blum

Dr. Ziad El Rassi

Dr. Jeffery White

Dr. Kaan Kalkan

Outside Committee Member

Dr. Sheryl Tucker

Dean of the Graduate College

TABLE OF CONTENTS

LIST OF TABLES

LIST OF FIGURES

Figure Page

Figure Page

CHAPTER I

INTRODUCTION

The term nanotechnology was first introduced in 1959 on a lecture on physics delivered by Professor Richard Feynman, entitled *There's Plenty of Room at the Bottom*.[1] Since the first introduction of nanotechnology, diverse definitions have emerged. Nanotechnology can be defined as the design, characterization, production, and application of structures, devices, and systems by controlled manipulation of size and shape at the nanometer scale (atomic, molecular, and macromolecular scale) that produces structures, devices, and systems with at least one novel/superior characteristic or property.[2] The materials obtained through manipulation of these properties are called nanomaterials.

One of the most promising elements used in nanoscale materials is carbon. Carbon is the sixth element in the periodic chart, yet one of the most important elements. It is located in the middle of the periodic table, and has the ability to form stable substances with the more electronegative or more electropositive ions. Even though its abundance in the Earth's crust is lower than many other terrestrial elements, carbon is essential for the formation of all organic matter.

Carbon has been known since the ancient times in the form of soot, charcoal, graphite and diamonds. It occurs in different forms of carbon, thus giving multiple allotropes or crystal structures. Depending on its structure, carbon has played important roles in human life for a long time. Charcoal, for example, has been known and used since ~5000 BC for various purposes such as in the manufacturing of bronze, a domestic fuel, an adsorbent, water purification, and medical treatment of a wide range of diseases. In the 20th century, activated carbon with controlled physical properties was widely developed and used in wartime due to its ability to adsorb poisonous gases that were under development and used in the battlefields.

A class of more recently-discovered carbon allotrope is the fullerenes. Unlike graphite that has a layered and planar structure where the carbon are arranged in hexagonal lattice , or diamond where carbon atom is bonded to four other carbon atoms by sp^3 bonds with cubic structure, in fullerenes, the sp^2 hybridized carbon has been arrange in a way to limit edges such as rolling into tubes or balls. Since their first discovery in 1985, fullerenes have been subjected to intensive investigations and promise a wide array of potential applications from drug delivery to energy conversions.[3-9] Fullerenes can come in different types, including spherical (called buckminsterfullerene or buckyballs), rods or tubes (called buckytubes or nanotubes), polymers, and onions (multiple carbon layers surrounding a buckyball core). The most common fullerene in terms of natural occurrence is buckminsterfullerene (C_{60}). Buckminsterfullerene is highly insoluble in water;[10] however, it can form stable colloidal aggregates upon contact with water variously called in the literature *n*C_{60}, nano-C_{60}, and fullerene water systems. The reported methods to disperse C_{60} in water include organic solvent exchange, dissolution in organic solvent followed by mixing with

water and driving off the organic solvent, and long-time stirring of C_{60} solids in water. Due to the wide range of conditions to disperse C_{60} in water, nano-C_{60} is readily available in natural systems. Research in nanomaterials related to carbon compounds, be they fullerenes, nanotubes or nanocrystalline diamond phases, is growing quickly in diverse areas, yet the environmental impacts of these materials are still largely unexplored.

The industrial scale manufacture and increased applications of fullerenes have raised safety concerns about C60. These concerns belong to a class of growing questions about the health and environmental impacts of engineered nanomaterials. Cytotoxicity of *n*C_{60} was initially reported in 2004.[11,12] These reports suggested that *n*C_{60} demonstrates the toxicity to several lines of cells in culture through an oxidative damage mechanism. In response to these initial findings, numerous reports confirmed[13-17] or contradicted[18-21] the reported cytotoxicity. Following the initial confusion, recent findings revealed that the decomposition product of tetrahydrofuran, an organic solvent often used in one of the preparation method of nano-C_{60}, is responsible for much of the oxidative damage initially observed, although the extent of this contribution is still under debate.[22-24] In the production of *n*C_{60} via tetrahydrofuran method, it is revealed that γ-butyrolactone and the degradation products of tetrahydrofuran were mainly responsible for the observed adverse effects of *n*C_{60} suspensions and elimination of these products by additional washing during THF/*n*C_{60} synthesis decreased the toxic effect to *D. magna* and A549 lung cells significantly.[24] Toxic effects of *n*C_{60} against several cell cultures from the previous studies were observed in treatments where tetrahydrofuran was used as an intermediate solvent to disperse C_{60} in water.[11,12] In these studies, the complete removal of tetrahydrofuran from the system was assumed and analysis of tetrahydrofuran or tetrahydrofuran degradation products was not performed. In the THF/*n*C_{60} method performed

by Henry *et al*, tetrahydrofuran removal was performed by sparging the samples with N_2 for 2.5 days subsequent to rotavaping to ensure tetrahydrofuran removal.[22] By this method, analysis using GC-MS showed that although no residual tetrahydrofuran was observed, its degradation products were present and can contribute to toxicity in THF/*n*C_{60}.

Since *n*C_{60} was reported to induce oxidative stress on the brain of juvenile largemouth bass,[11] several studies have shown more evidence that fullerenes could migrate throughout mice bodies and accumulate in the mouse livers, in lysosomes, cytoplasm, along the plasma membrane, and inside the nucleus of human monocyte macrophages.[25-27] In contrast to these results, Sinohara *et al*[21] reported that very few or no *n*C_{60} aggregates reached the brain of *C. carpio* across the blood-brain barrier and no lipid peroxidation was induced in their brains. Up to this point, the understanding of C_{60} toxicity and bioactivity remains limited due to the various experiment conditions and the complexity of *n*C_{60} systems, which as a consequence, had different size, shape and charge among reported results. In the recent study by Song *et al.*[28], it is reported that toxicity of *n*C_{60} may be influenced by the size and aggregation state of the particles. By using fractions of *n*C_{60} aggregates with different size distributions prepared by a simple differential centrifugation, they demonstrate the size-dependent inhibition of DNA polymerase and reduced-size enhanced cytotoxicity. It is reported that *n*C_{60} aggregates with smaller sizes may have higher toxicity potency, where the size-dependent effects were observed at the high exposure doses (4–6 mg/L).[28]

Purpose of study

The significant differences in the physicochemical properties of the resulting *n*C_{60} colloidal suspensions among the reported synthesis methods make it important to understand clearly

the properties of the samples produced under the conditions that are least-likely to have contaminants resulting from organic solvents: the simple long-term stirring in water termed aqu/*n*C_{60} method. Considering that C_{60} is hydrophobic, it should not be soluble in water. However, its ability to form water-stable aggregates by a wide range of methods motivates the need to understand clearly the factors that allow the fullerene colloids to be stably dispersed in water. A second objective is to evaluate the oxidative behavior of *n*C_{60} prepared using the controversial solvent, tetrahydrofuran, as compared to less problematic solvents such as toluene.

This dissertation is divided into five chapters. The statement of the problem and the purpose of study are discussed in Chapter I. The literature review on C_{60}, aqueous C_{60} colloidal suspensions, and their toxicity controversies are discussed in Chapter II. Approaches used to answer the factors that allow the fullerene colloids to be stably dispersed in water and the preliminary study of the oxidative behavior of *n*C_{60} are discussed in Chapter III and IV, respectively. Conclusions from these studies are discussed in Chapter V.

References

1. Feyman, R. P. in *Miniaturization* (ed Horace D. Gilbert) 282 - 296 (Reinhold Publishing Corporation, 1961).
2. Bawa, R., Bawa, S. R., Maebius, S. B., Flynn, T. & Wei, C. Protecting new ideas and inventions in nanomedicine with patents. *Nanomedicine* **1**, 150-158, (2005).
3. Haddon, R. C., Hebard, A. F., Rosseinsky, M. J., Murphy, D. W., Duclos, S. J., Lyons, K. B., Miller, B., Rosamilia, J. M., Fleming, R. M., Kortan, A. R., Glarum, S. H., Makhija, A. V., Muller, A. J., Eick, R. H., Zahurak, S. M., Tycko, R., Dabbagh, G. & Thiel, F. A. Conducting Films of C60 and C70 by Alkali-Metal Doping. *Nature* **350**, 320-322, (1991).
4. Innocenzi, P. & Brusatin, G. Fullerene-based organic-inorganic nanocomposites and their applications. *Chem Mater* **13**, 3126-3139, (2001).
5. Kelty, S. P., Chen, C. C. & Lieber, C. M. Superconductivity at 30-K in Cesium-Doped C60. *Nature* **352**, 223-225, (1991).
6. Ruoff, R. S. & Ruoff, A. L. Is C60 Stiffer Than Diamond. *Nature* **350**, 663-664, (1991).
7. Sariciftci, N. S., Smilowitz, L., Heeger, A. J. & Wudl, F. Photoinduced Electron-Transfer from a Conducting Polymer to Buckminsterfullerene. *Science* **258**, 1474-1476, (1992).
8. Tsao, N., Kanakamma, P. P., Luh, T. Y., Chou, C. K. & Lei, H. Y. Inhibition of Escherichia coli-induced meningitis by carboxyfullerence. *Antimicrob Agents Ch* **43**, 2273-2277, (1999).
9. Ungurenasu, C. & Airinei, A. Highly Stable C60/Poly(vinylpyrrolidone) Charge-

Transfer Complexes Afford New Predictions for Biological Applications of Underivatized Fullerenes. *J. Med. Chem.* **43**, 3186 - 3199, (2000).

10. Korobov, M. V. & Smith, A. L. in *Fullerenes: Chemistry, Physics, and Technology* (eds K. M. Kadish & R. S. Ruoff) 60 (John Wiley and Sons, Inc., 2000).

11. Oberdorster, E. Manufactured nanomaterials (Fullerenes, C-60) induce oxidative stress in the brain of juvenile largemouth bass. *Environ Health Persp* **112**, 1058-1062, (2004).

12. Sayes, C. M., Fortner, J. D., Guo, W., Lyon, D., Boyd, A. M., Ausman, K. D., Tao, Y. J., Sitharaman, B., Wilson, L. J., Hughes, J. B., West, J. L. & Colvin, V. L. The differential cytotoxicity of water-soluble fullerenes. *Nano Lett* **4**, 1881-1887, (2004).

13. Dhawan, A., Taurozzi, J. S., Pandey, A. K., Shan, W., Miller, S. M., Hashsham, S. A. & Tarabara, V. V. Stable colloidal dispersions of C60 fullerenes in water: evidence for genotoxicity. *Environ Sci Technol* **40**, 7394-7401, (2006).

14. Lyon, D. Y. & Alvarez, P. J. Fullerene water suspension (nC60) exerts antibacterial effects via ROS-independent protein oxidation. *Environ Sci Technol* **42**, 8127-8132, (2008).

15. Sayes, C. M., Gobin, A. M., Ausman, K. D., Mendez, J., West, J. L. & Colvin, V. L. Nano-C-60 cytotoxicity is due to lipid peroxidation. *Biomaterials* **26**, 7587-7595, (2005).

16. Zhu, S. Q., Oberdorster, E. & Haasch, M. L. Toxicity of an engineered nanoparticle (fullerene, C-60) in two aquatic species, Daphnia and fathead

minnow. *Mar Environ Res* **62**, S5-S9, (2006).

17. Zhu, X., Zhu, L., Lang, Y. & Chen, Y. Oxidative stress and growth inhibition in the freshwater fish Carassius auratus induced by chronic exposure to sublethal fullerene aggregates. *Environ Toxicol Chem* **27**, 1979-1985, (2008).
18. Andrievsky, G., Klochkov, V. & Derevyanchenko, L. Is the C-60 fullerene molecule toxic?! *Fuller Nanotub Car N* **13**, 363-376, (2005).
19. Gharbi, N., Pressac, M., Hadchouel, M., Szwarc, H., Wilson, S. R. & Moussa, F. [60]fullerene is a powerful antioxidant in vivo with no acute or subacute toxicity. *Nano Lett* **5**, 2578-2585, (2005).
20. Levi, N., Hantgan, R. R., Lively, M. O., Carroll, D. L. & Prasad, G. L. C60-fullerenes: detection of intracellular photoluminescence and lack of cytotoxic effects. *J Nanobiotechnology* **4**, 14, (2006).
21. Shinohara, N., Matsumoto, T., Gamo, M., Miyauchi, A., Endo, S., Yonezawa, Y. & Nakanishi, J. Is lipid peroxidation induced by the aqueous suspension of fullerene C60 nanoparticles in the brains of Cyprinus carpio? *Environ Sci Technol* **43**, 948-953, (2009).
22. Henry, T. B., Menn, F. M., Fleming, J. T., Wilgus, J., Compton, R. N. & Sayler, G. S. Attributing effects of aqueous C60 nano-aggregates to tetrahydrofuran decomposition products in larval zebrafish by assessment of gene expression. *Environ Health Perspect* **115**, 1059-1065, (2007).
23. Kovochich, M., Espinasse, B., Auffan, M., Hotze, E. M., Wessel, L., Xia, T., Nel, A. E. & Wiesner, M. R. Comparative toxicity of C60 aggregates toward mammalian cells: role of tetrahydrofuran (THF) decomposition. *Environ Sci*

Technol **43**, 6378-6384, (2009).

24. Spohn, P., Hirsch, C., Hasler, F., Bruinink, A., Krug, H. F. & Wick, P. C-60 fullerene: A powerful antioxidant or a damaging agent? The importance of an in-depth material characterization prior to toxicity assays. *Environ Pollut* **157**, 1134-1139, (2009).

25. Porter, A. E., Muller, K., Skepper, J., Midgley, P. & Welland, M. Uptake of C60 by human monocyte macrophages, its localization and implications for toxicity: studied by high resolution electron microscopy and electron tomography. *Acta Biomater* **2**, 409-419, (2006).

26. Porter, A. E., Gass, M., Muller, K., Skepper, J. N., Midgley, P. & Welland, M. Visualizing the uptake of C60 to the cytoplasm and nucleus of human monocyte-derived macrophage cells using energy-filtered transmission electron microscopy and electron tomography. *Environ Sci Technol* **41**, 3012-3017, (2007).

27. Oberdorster, G., Oberdorster, E. & Oberdorster, J. Nanotoxicology: An emerging discipline evolving from studies of ultrafine particles. *Environ Health Persp* **113**, 823-839, (2005).

28. Song, M., Yuan, S., Yin, J., Wang, X., Meng, Z., Wang, H. & Jiang, G. Size-dependent toxicity of nano-C60 aggregates: more sensitive indication by apoptosis-related Bax translocation in cultured human cells. *Environ Sci Technol* **46**, 3457-3464, (2012).

CHAPTER II

REVIEW OF LITERATURE

Discovery and Productions of Fullerenes

Fullerenes are allotrope of carbon like graphite, diamond and amorphous carbon. It is an all-carbon molecule in the form of a hollow sphere, tube, or ellipsoid. The existence of fullerenes was theoretically predicted in the year 1970 by Eiji Osawa from Toyohashi University of Technology.[1] While working on superaromatic π–systems, he postulated a soccer-ball-structure with icosahedral symmetry for the C_{60} molecule, rather than a long chain, based on its stability from Hückel calculations. In the same year, a scientist from the Atomic Energy Research Establishment in the United States, R. W. Henson, proposed the structure of C_{60}, but unfortunately the evidence for this new form of carbon was too weak and was not accepted.[2]

In the year 1985, the hollow-sphere fullerene, termed buckyball or buckminsterfullerene or fullerene (C_{60}) , was discovered by Richard Smalley and Robert Curl from Rice University and Harold Kroto from the University of Sussex.[3] The name fullerene was derived from Buckminster Fuller, whose geodesic architectural structures resemble the proposed shape of fullerene.

Fullerenes are produced in nature as a component of soot and normally formed by lightning discharges in the atmosphere. In the experimental investigation by Kroto *et al.*,[3] C_{60} was produced by firing a high energy laser beam at a rotating disk of graphite in a helium-filled chamber. The intense heat applied on the surface of the graphite broke the C–C bonds due to the intense energy. Carbon species were then vaporized and condensed in high-pressure helium gas. Immediately upon cooling, the carbon was introduced to a mass spectrometer for analysis.

The method used by Kroto, *et al.*, to produce C_{60} resulted in yields of C_{60} only sufficient for mass spectrometry analysis. In the year 1990, Kratschmer, *et al.*, reported a new technique to synthesize C_{60} in gram quantities, allowing more detailed analysis of the compound.[4] Even though the soot produced from this method only contained 10 – 15% yield of C_{60}, it could easily be extracted into benzene or toluene. In their report, it was confirmed that the C_{60} molecules have a hexagonal close packing of soccer-ball-shape and have a "fullerene" structure.

Partial combustion of hydrocarbons under suitable conditions may also result not only soot, but also fullerenes. Benzene is the most common source of carbon for this process, where it is mixed with oxygen and argon and burned in a laminar flame. The resulting mixture contains soot, polycyclic aromatic compounds and certain fractions of fullerenes that make up 0.003 – 9.0% of the soot's total mass. Other hydrocarbon such as toluene or methane may be employed as the source of carbon as well.

Under suitable reaction conditions, hydrocarbon combustion can yield an increase portion of C_{70} in the fullerene soot, with up to 80% of fullerenes are obtained. The ratio of C_{70}/C_{60} seems to be influenced by the gas pressure, where the fraction of C_{70} increases

with increasing pressure. Currently, hydrocarbon combustion is the only commercial method in use to prepare large amounts of C_{60}. A plant producing approximately 500 tons of fullerenes per year using benzene combustion has recently in operation in Japan.[5]

Properties of Fullerene

Fullerene C_{60} has a soccer ball shape with 60 vertices and 32 faces, consists of 20 hexagons and 12 pentagons. It has 120 symmetry operations (e.g. rotation around the axis and reflection in a plane), which makes it the most symmetrical known molecule.[6] Each carbon atom in C_{60} is covalently bonded to three carbon atoms forming conjugated double bonds as shown in Figure 2.1.

There are two distinct types of bonds in C_{60}, the [6,6]- and the [5,6]-bonds. The [6,6]-bonds can be found at the edge between two hexagons, while the [5,6]-bonds between the hexagons and pentagons. The bond lengths for [6,6]- and [5,6]-bonds are 135.5 pm and 146.7 pm respectively, and thus, [6,6]-bond has more pi bond character. Despite the high degree of conjugation, C_{60} behaves chemically and physically as an electron-deficient alkene rather than as an electron-rich aromatic system.[7]

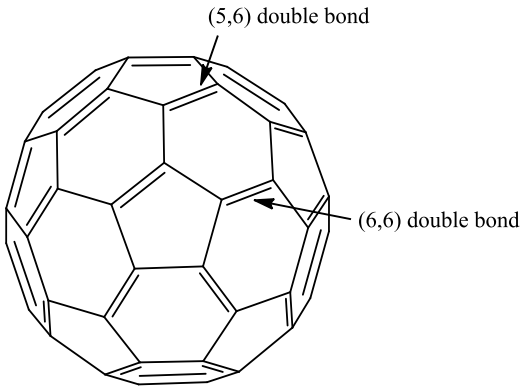

Figure 2.1 Structure of fullerene C_{60}

Physical Properties of Fullerene

C_{60} is a very hydrophobic molecule, and thus cannot be dissolved in polar solvents. It is sparingly soluble in alkanes with solubility increasing as the length of the hydrocarbon chain increases, but is generally soluble in aromatic solvents and carbon disulfide[8] due to the $\pi - \pi$ interactions. C_{60} is highly electronegative and readily acts as an electron acceptor in charge-transfer complexes. As a result, C_{60} can easily be dissolved by solvents that provide a free pair of electrons. Solubility of C_{60} thus increases in aromatic solvents with electron donating atoms such as pyridine. The comparison of benzene with its saturated analog, cyclohexane, is an impressive example where the solubility reaches 1.4 mg/L versus 0.036 mg/L, respectively, due to the aromatic molecule's electron density.[5] Inorganic solvents exhibit the same trend: solubility of C_{60} increases in substances that can form donor-acceptor complexes.

The absorption spectrum of C_{60} is characterized by strong absorptions between 190 to 410 nm, as well as by weaker transitions in the visible part of the spectrum.[8,9] The strong absorptions for C_{60} lie at 213, 257 and 329 nm and there is an interesting weak band, which is unusually sharp, at 404 nm.[10] The band at 213 nm has a shoulder at 227 nm and that at 329 nm has several distinguishable shoulders at 365, 377, 391, and 396 nm. The absorptions between 190 and 410 nm are due to allowed ${}^1T_{1u} \rightarrow {}^1A_g$ transitions, while the absorptions between 410 and 620 nm are due to various forbidden singlet-singlet transitions, which gives the characteristic purple color of C_{60} in solutions.[8] The absorption spectrum of C_{60} in toluene from 300 – 800 nm is shown in Figure 2.2.

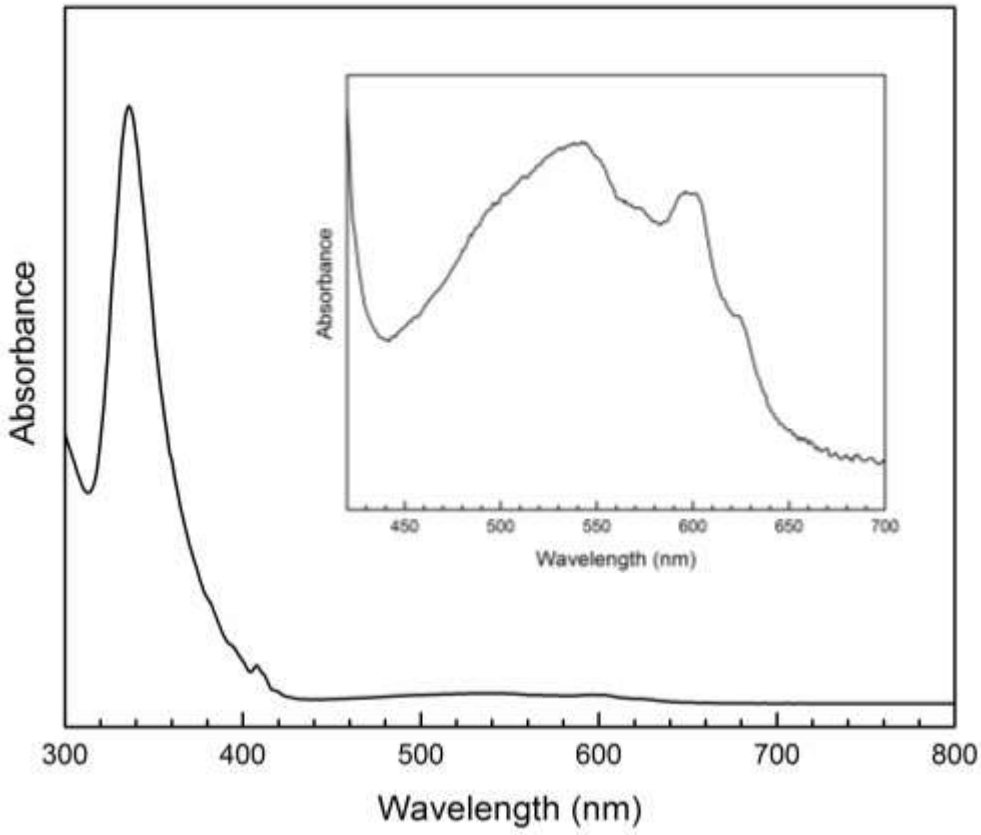

Figure 2.2 Electronic absorption spectrum of C_{60} in toluene. The inset is the 420 – 700 nm region.

When there is a change of aromatic solvent used to dissolve C_{60}, the difference in the strong absorptions is mainly observed spectroscopically by a bathochromic shift of the 239 nm band. These changes most likely result from a charge-transfer interaction of the electrophilic fullerene with the solvent's π-system.[5]

Solid C_{60} is a van der Waals crystal. In the solid state, C_{60} retains features of the molecular absorption spectrum. In the longer wavelength region, specifically in the 420 to 520 nm, there is a large difference between the solution and solid spectrum. The band at 445 nm with a shoulder around 495 nm is very much enhanced in intensity for the solid

state.[11] The absorption in this wavelength range is assigned to transitions associated with a parity-forbidden HOMO-LUMO gap ($h_u - t_{1u}$).[11] For nanoparticles, in the longer wavelength region between 420 – 520 nm, the same absorption band as found in C_{60} solid state is also observed.

C_{60} has 174 vibrational modes, of which 42 are distinct. Only four modes are of t_{1u}-symmetry rendering them IR-active.[5] Fourier transform infra-red (FTIR) spectra of C_{60} show these four bands at 1430, 1182, 577, and 527 cm^{-1} as expected from symmetry considerations.

^{13}C-NMR spectroscopy of C_{60} is also dominated by symmetry considerations, since all sixty carbon atoms are equivalent. The single observed peak is found at 143.2 ppm (using d_6-benzene as a solvent), located within a shift region characteristic of electron deficient olefins rather than at a typical aromatic values, further supporting the molecule's relatively low aromatic character.[5]

Chemical Properties of Fullerene

As expected from the hollow shape of C_{60}, there is a general differentiation between the outside and inside reactivity. Modification of the outside surface of C_{60} is termed exohedral functionalization, where the modifications are performed by decorating the C_{60} surface with one or more functional groups, attached to the carbon atoms. This modification process can be divided into covalent and non-covalent interactions between C_{60} and the functional groups. Modification of the inside surface of C_{60} is termed endohedral functionalization, where small molecules or atoms are included in the cavity within the C_{60} cage. Due to the extreme conformational strain that would be required in the fullerene cage, there are no observed examples of endohedral covalent

functionalization of C_{60}. Even a single nitrogen atom, when forced inside the C_{60} cage, rests centrally within the cavity, not bonding to the surrounding carbon atoms.[5]

Chemical reactions involving C_{60} can be classified into several major categories such as reduction and oxidation, addition, polymerization, and host-guest complexing.[12] The high electron affinitiy of C_{60} strongly favors its reduction relative to its oxidation, leading to anion formation of C_{60}^{n-}. Many of the reduction reactions of C_{60} have been made with alkali and alkaline earth metals.

The C_{60} derivatization can be obtained by hydrogenation and alkylation reactions. Hydrogenated derivatives of C_{60} have been synthesized through chemical, electrochemical and catalytic methods. Birch reduction, for example, has been used to prepare $C_{60}H_{18}$ and $C_{60}H_{36}$ where lithium metal is used in the presence of *t*-butanol to reduce the C_{60} to the monoanion C_{60}^{-} which then followed by hydrogen attachment.[13]

Addition reactions using C_{60} can be categorized into Diels-Alder cycloadditions, additions involving bridging, halogenation, addition of nucleophiles such as reaction with amines, and addition of radicals.[12] Hydroxyl groups can also be added to C_{60} by addition of nitronium ion, followed by nucleophilic replacement by OH to produce fullerols.[14] Fullerols produced by this method contain about 18 hydroxyl groups. Reactions of fullerols formation are likely to be studied intensively due to the water-solubility of the products and the possibility of cage-opening reactions.

One of the main processes used to modify the surface of C_{60} exohedrally that is relevant to the studies in the next chapters is oxidation reaction using molecular oxygen to yield $C_{60}O$. Photo-oxidation reaction in the presence of molecular oxygen can also yield $C_{60}O$ through a reaction between the first excited singlet state of C_{60} with singlet

oxygen. In this reaction, oxygen is added to the 6,6-double bond to form an epoxide of $C_{60}O$. In addition to the epoxidic structure of oxides, another species is conceivable that features an opened ring and a cyclic ether functionality.[5] Reaction of C_{60} with ozone generates ozonides which further dissociate through two different pathways: thermolysis and photolysis, as shown in Figure 2.3. In the former, the epoxide is obtained, and in the latter, oxidoannulene, the opened ring isomer of oxide with the oxygen added to the 5,6-bond is obtained. The reaction of C_{60} with ozone is vigorous that higher number of oxides may be obtained to produce $C_{60}O_n$ where $n > 1$, as shown in Figure 2.4.

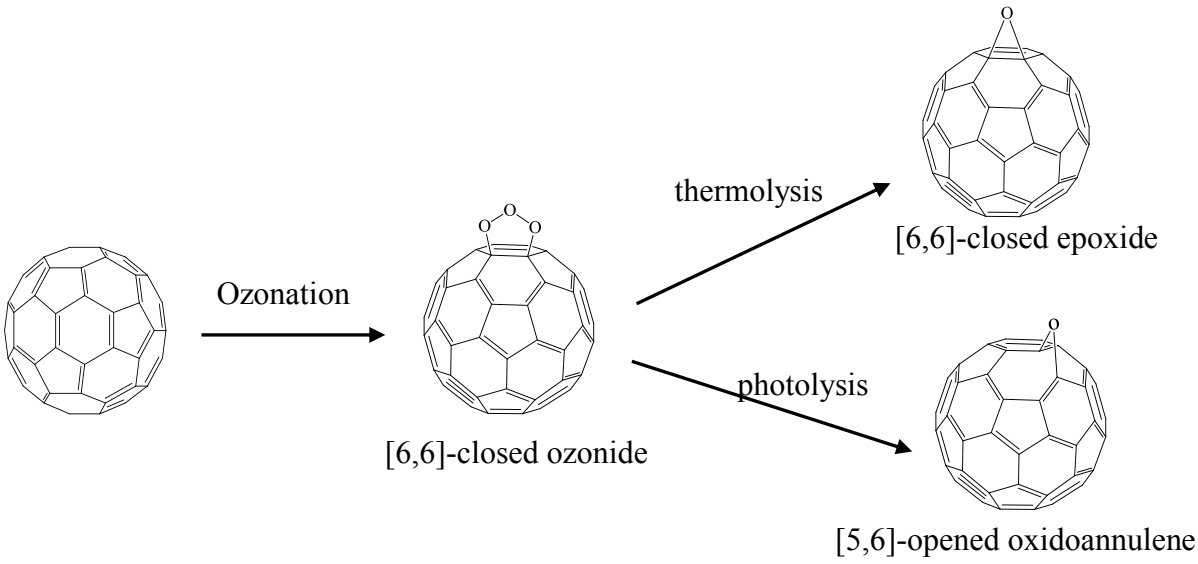

Figure 2.3. Oxidation reaction of C_{60} with ozone.

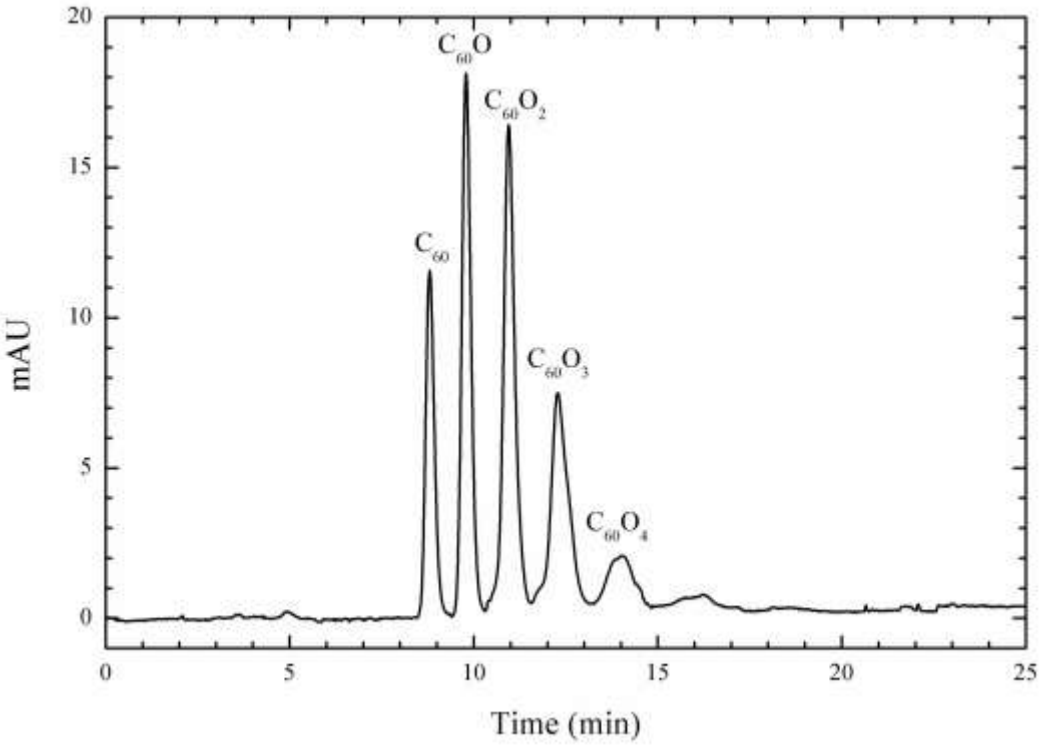

Figure 2.4. HPLC profile of reaction of C_{60} in toluene with ozone producing higher number of oxides

Electronic and Optical Properties of C_{60}

Photophysics of C_{60} has been previously reported and reviewed.[15-17] The electronic and optical properties of C_{60} can be described using a Jablonski diagram as shown in Figure 2.5[18] A molecule in the S_0 (singlet ground state) can absorb light efficiently and promote an electron to an excited singlet state. Once promoted into an excited singlet state, a molecule will undergo rapid radiationless decay to the S_1 (lowest excited singlet state). During this process, the difference in electronic state energies are converted into vibrational excitation, and the excited molecule may further relax to S_0 by fluorescence emission or nonradiatively decay to S_0 through an internal conversion (IC), or to a triplet state through an intersystem crossing (ISC). Unimolecular electronic decay of T_1 to S_0

then normally occurs through phosphorescence photon emission (a process that is generally negligible for C_{60}), and $T_1 \rightarrow S_0$ intersystem crossing. In the most common fullerenes, the dominant decay sequence after optical excitation is IC from S_n to S_1, followed by ISC and IC from S_1 through T_n to T_1.[18] . These processes from S_0 to T_1 happen too quickly for bimolecular process to be important. In the absence of later bimolecular processes, the T_1 state has a lifetime dominated by ISC from T_1 back to S_0. Thus, the T_1 state is the photophysical state that is important for all bimolecular processes. The most important bimolecular process that is relevant to the study in the next chapters is oxygen quenching. The triplet state of C_{60} is easily quenched by molecular oxygen to produce singlet oxygen ($^1O_2$) and ground state C_{60}.

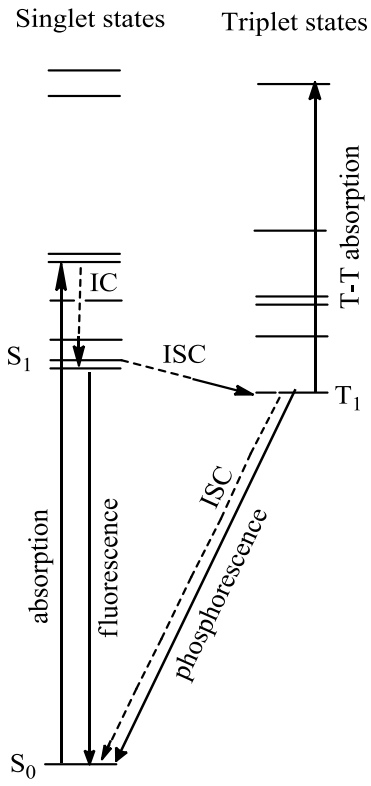

Figure 2.5 Electronic energy-level diagram showing radiative and nonradiative transitions.

Applications of Fullerenes

Since its discovery in 1985, C_{60} has been extensively studied due to its unique properties and wide range of potential applications from medical purposes to solar cells. Although C_{60} itself is not soluble in water, many derivatives of C_{60} can be very water soluble. Solubilization of C_{60} using cyclodextrin or calixerenes has been reported[19,20], as well as other solubilization methods such as using detergents, phospholipids, micelles, etc.[21-24]

Derivatives of C_{60} have been investigated for medical purposes such as antiviral activities, antioxidant activities, and drug delivery. C_{60} and its derivatives have potential antiviral activity, which has strong implications on the treatment of HIV-infections.[25] Derivatives of C_{60} have been shown to make complex with HIV protease (HIV-P) and act as an inhibitor.[26,27] Dendrofullerenes (C_{60}DF), which are soluble in water, have been reported to have the highest anti-protease activity.[28,29] Fulleropyrrolidines with two ammonium groups and C_{60} derivatized with two or more solubilizing side chains have been reported to be active against HIV-1 and HIV-2. [30,31] Amino acid derivatives of C_{60} have also been shown to inhibit HIV and human cytomegalovirus replication.[32] Other antiviral actions of C_{60} have also been reported, for example enveloped viruses in blood that can be inactivated by C_{60} in the presence of O_2 and light through photodynamic reactions.[33]

Inorganic nanoparticles such as C_{60} have been considered to be potential carriers to transport gene or drugs due to their small size (~1 nm) and biocompatibility. Although the C_{60} core is highly hydrophobic, by attaching hydrophilic moieties to the core, C_{60} becomes soluble in water and is able to carry drugs and genes for cellular delivery.

Derivatization of fullerene surfaces have the potential to provide a lipophilic slow-release drug delivery system, which can enhance the therapeutic efficacy in tissue, as reported by Zakharian, *et al*.[34]

Due to the fact that C_{60} is highly conjugated and has a low lying LUMO that can easily take up to six electrons, it can act as an effective radical scavenger or radical sponge.[35] Such radical scavengers have been shown to protect cell growth from various toxins that can induce apoptotic injuries *in vitro* [36-38] in different cell types including neuronal cells, hepatoma cells, or epithelial cells.[25,39-42] Due to their propensity to generate singlet oxygen, fullerenes have been considered as photosensitizers (PS) for photodynamic therapy (PDT).[16,43] PDT relies on the administration of a PS to a lesion, followed by the illumination of the lesion with visible light to activate the PS. In the presence of oxygen, activation of PS leads to the generation of reactive oxygen species and consequently to cell death. Pristine or functionalized fullerenes have been reported to be used in PDT applications such as cleavage of DNA strands,[44-46] oxidative damage to the lipid membranes,[47-49] photoinactivation of viruses[33,50-52] and microbes,[53,54] phototoxicity of cancer cells,[55,56] and photodynamic therapy of tumors.[57,58]

C_{60} has a high electron affinity and the ability to transport electrons effectively. Due to its unique electronic properties, C_{60} has been considered to be used in a number of electronic-related devices from data storage to solar cells. Because C_{60} has a small energy gap between the HOMO and LUMO orbitals, C_{60} can be easily tuned as a good conductor. Transport measurements show that C_{60} is a semiconductor with a very high resistivity, however, by doping C_{60} with alkali metals, alkali-earth metals, and various organic electron donors, the resulting charge transfers greatly reduce the resistivity and in

some cases can yield metallic conduction.[59] Haddon, *et al.*, were the first to report in their study that electronic properties of C_{60} were greatly modified after intercalating alkali metals into C_{60} to a stoichiometry M_3C_{60}, where *M* = *K*, *Rb*, and *Cs*. The discovery of the unusual optical transport and electronic properties of C_{60} further raised research activities in the field of C_{60}-related materials to investigate the possible applications as photoconductors, diode rectifiers, optical limiters, photorefractive materials, etc.

Aqueous C_{60} Colloidal Suspensions

Due to these unusual properties of C_{60} and the extensive research concerning their potential applications, C_{60} is now being produced in multi-ton quantities to supply it at a reasonable price so as to make it a practical material for industrial applications.[60] This increase in production has resulted in a corresponding increase in studies addressing its potential environmental and biological impacts. Solubility of C_{60} in water has gained higher attention after the bioactivity of C_{60} was observed in the early 1990s. Methods to solubilize C_{60} in water were soon under investigations. The low solubility of C_{60} in water (< 10^{-9} mg/L) is well accepted.[61] However, upon contact with water, C_{60} can aggregate and form stable colloidal suspensions in water, variously called fullerene-water-system, nano-C_{60}, and *n*C_{60} in the literature.[62-67]

There are five different reported methods to disperse C_{60} in water, which classified into three groups. They are sonication methods,[62,63,66] organic solvent exchange, such as THF, TTA, HIPA and HEA methods (described below),[64,66,68] and simple long-time stirring of C_{60} powder in water (also known as the aqua method).[66,67]

The five different reported methods to disperse C_{60} in water are briefly described as follow:

1. SON/*n*C_{60}: the use of ultrasound assists the transfer of fullerene from toluene to water. Sonication method gives extremely high colloid concentration compared to other methods. This approach also has a least controlled condition throughout the process. High temperature and pressure were produced during the process which causes a wide range of chemical reactions and producing the largest distribution of particle size as compared to other synthetic methods.
2. THF/*n*C_{60}: this method involves a mechanical mixing of C_{60} in tetrahydrofuran (THF) with the addition of water, follows by the evaporation of the organic solvent from the system using rotary evaporator.[63,66] Even though this approach is easy to reproduce with controlled particle size, it has produced controversy concerning toxicological studies, due to some disagreements whether tetrahydrofuran or the autoxidation products that might interfere significantly to cause toxicity.[69]
3. TTA/*n*C_{60}: this method involves a gradual transfer from a "good" solvent (toluene) to a "bad" solvent (water) through intermediate solvents (tetrahydrofuran and acetone).[64,66] Compared to all reported synthesis method, this approach gives the most controlled particle growth and smallest particle size. The disadvantage of this method is the use of tetrahydrofuran as one of the intermediate solvents. Another downside of this method is that the combination of solvents used (toluene/benzene, tetrahydrofuran, acetone) have relative vapor-pressure in the opposite order of their solubility. As the solvents are removed

from the mixture, the "poor" solvents are removed before the "good" solvents. This results in an increase instead of a decrease of solubility during evaporation. Close to the end of the TTA synthesis method, the C_{60} remains in the toluene layer above the aqueous layer and because of the different solubility of C_{60} in the two layers, at the end of the evaporation of toluene, the majority of C_{60} particles are too large to be suspended in water and prefer to precipitate out of the suspensions. As a result, the concentration of nC_{60} obtained by this procedure is significantly decreased.

4. HIPA/nC_{60} and HEA/nC_{60}: these methods involve gradual transfer from a "good" solvent (hexane) to a "bad" solvent (water) through intermediate solvent (ethanol and isopropanol for HEA and HIPA, respectively)[68] similar to TTA/nC_{60}, with some advantages as compared to TTA/nC_{60}. In HIPA and HEA, the use of the controversial solvent tetrahydrofuran is avoided. In this procedures also, the solubility and vapor-pressure are in the same order, which results in a decrease of solubility of C_{60} in the solvents during evaporation.
5. AQU/nC_{60}: this technique involves a long-term mixing of C_{60} in water for a period of days to months without the presence of organic solvent.[66,67] Even though this method is the most environmental friendly due to the absence of organic solvents, the disadvantage of this method is its low percent yield and long preparation time.

Due to this tendency to form stable suspensions, nC_{60} is potentially readily available in natural systems, and the toxicity of this nanomaterial has become of great interest.

Toxicity Controversies

In 2004, it was first reported that C_{60} colloidal suspensions in water (termed *n*C_{60}) exhibits severe cytotoxicity to several cell lines in culture through an oxidative damage mechanism.[70,71] Oberdörster reported that the uncoated *n*C_{60} caused significant increase of lipid peroxidation in the brain and glutathione (GLH) depletion in the gill of largemouth bass after 48 hours of exposure to 0.5 ppm uncoated *n*C_{60}.[70] Following this report, Sayes, *et al.*,[71] also reported that *n*C_{60} was substantially more toxic than highly soluble derivatives such as $C_{60}(OH)_{24}$. In their study, oxidative damage to the cell membranes was observed where fullerene exposure led to cell death. This study also showed that under ambient conditions in water fullerenes can generate superoxide anion, which was postulated to be responsible for membrane damage and subsequent death. Both Oberdörster and Sayes studies used *n*C_{60} prepared via solvent exchange method to disperse the C_{60} in water, by initially dissolving C_{60} in tetrahydrofuran, mixing it with water, and followed by evaporating of the organic solvent.

In response to these initial findings, numerous reports confirmed[72-76] or contradicted[77-80] this reported cytotoxicity. Andrievsky, *et al.*, in their study claimed that the use of *n*C_{60} prepared using solvent exchange method should not be used for biological tests due to many reasons such as the composition of dispersed particles, its size distribution was difficult to reproduce, and the particles contained a lot of both organic solvent and other impurities that could ultimately distort the true biological properties of pristine C_{60}.[77] The reports that confirmed the reported cytotoxicity of *n*C_{60} used suspensions prepared via solvent exchange method by initial dissolution of C_{60} in

tetrahydrofuran or ethanol. Even though the initial proposed mechanism for this cytotoxicity was through lipid peroxidation by the presence of reactive oxygen species (ROS), Lyon and Alvarez[73] reported that the oxidation stress in the mammalian cell by nC_{60} requires direct contact between the nanoparticle and the bacterial cell. This report suggested that the mechanism of oxidative behavior by nC_{60} was obtained through non-ROS generating pathway.

A study by Henry, *et al.*,[81] revealed that the oxidative damage initially observed in largemouth bass by Oberdorster[70] can be contributed by the presence of decomposition products from tetrahydrofuran that had been used in several of the syntheses of the aqueous colloids. γ-butyrolactone, which was observed to be present in the THF/nC_{60} preparation, was shown to be acutely toxic at low concentrations. In their study, THF/nC_{60} was found to be more toxic than THF/water based on larval zebrafish survival and gene expression pattern.[81] This study also confirmed that the concentration of γ-butyrolactone was higher in THF/nC_{60} as compared to in THF/water, which could have resulted from differences in evaporation of water during preparation, or, perhaps, the presence of C_{60} enhanced the formation of γ-butyrolactone.[81] This report demonstrates that there are significant differences in the physical and chemical properties of the resulting nC_{60} colloidal suspensions among the reported synthesis methods. To follow this finding, Sphon, *et al.*,[82] reported in their study that ROS induction in A549 cells was not observed when aqu/nC_{60} was introduced to the system. This result contradicted the result of Oberdörster[70] and Sayes, *et al.*, where they used THF/nC_{60} in their control studies. On the contrary, THF/nC_{60} led to a 3.5-fold increase in ROS production when applied to the A549 cells. In order to confirm whether or not tetrahydrofuran is the

species responsible for induce ROS formation, Sphon *et al* applied different concentration of tetrahydrofuran (ranging from 100 to 1600 ppm) directly to the A549 cells. The negative results indicating that tetrahydrofuran itself was not able to induce ROS formation. Another study was performed using the first wash water from the synthesis of THF/*n*C_{60}, where they observed double ROS formation as compared to untreated cells. This indicates that the possible toxic side product was transferred to the wash water. In the solid-phase microextraction (SPME) GC-MS analysis, they observed the presence of 2-hydroxytetrahydrofuranol and some minor residue of tetrahydrofuran. In the mock treated tetrahydrofuran suspension, where it is lacking only the C_{60}, they also observed that 2-hydroxytetrahydrofuran was present as a major component but did not contain residual tetrahydrofuran, which explained that the remaining tetrahydrofuran in THF/*n*C_{60} suspensions might be due to the intercalation of tetrahydrofuran into *n*C_{60} agglomerates.[77] Sphon, *et al.*, also observed a potential increased level of highly active tetrahydrofuran hydroperoxide, a well-described oxidation product of tetrahydrofuran, as shown in Figure 2.6. Tetrahydrofuran is known to be easily oxidized, where tetrahydrofuran hydroperoxide is formed as a first intermediate. The hydroperoxide can further undergo hemolytic cleavage to γ-butyrolactone, a water soluble compound that can be eliminated by additional wash-step.

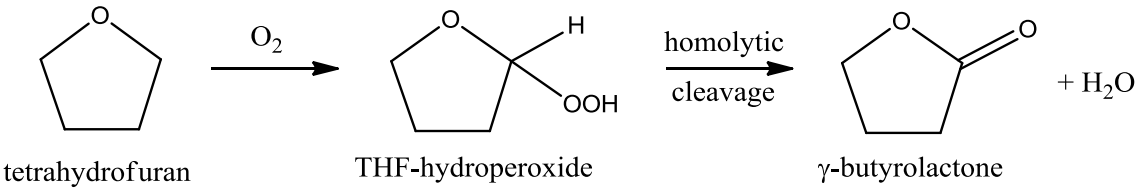

Figure 2.6 Possible scheme of tetrahydrofuran producing a side reaction.[82]

References

1. Osawa, E. *Kagaku* **25**, 854, (1970).
2. Thower, P. A. Novel carbon materials - What if? (editorial). *Carbon* **37**, 1667 - 1668, (1999).
3. Kroto, H. W., Heath, J. R., Obrien, S. C., Curl, R. F. & Smalley, R. E. C-60 - Buckminsterfullerene. *Nature* **318**, 162-163, (1985).
4. Kratschmer, W., Lamb, L. D., Fostiropoulos, K. & Huffman, D. R. Solid C-60 - a New Form of Carbon. *Nature* **347**, 354-358, (1990).
5. Krueger, A. *Carbon Materials and Nanotechnology*. (Wiley-VCH Verlag GmbH & Co., 2010).
6. Taylor, R., Hare, J. P., Abdulsada, A. K. & Kroto, H. W. Isolation, Separation and Characterization of the Fullerenes C-60 and C-70 - the 3rd Form of Carbon. *J Chem Soc Chem Comm*, 1423-1424, (1990).
7. Fowler, P. W. & Ceulemans, A. Electron Deficiency of the Fullerenes. *J Phys Chem-Us* **99**, 508-510, (1995).
8. Hirsch, A. *The chemistry of the fullerenes*. (Georg Thieme, 1994).
9. Kato, T., Kodama, T., Shida, T., Nakagawa, T., Matsui, Y., Suzuki, S., Shiromaru, H., Yamauchi, K. & Achiba, Y. Electronic Absorption-Spectra of the Radical-Anions and Cations of Fullerenes - C60 and C70. *Chem Phys Lett* **180**, 446-450, (1991).
10. Hare, J. P., Kroto, H. W. & Taylor, R. Preparation and Uv Visible Spectra of Fullerenes C60 and C70. *Chem Phys Lett* **177**, 394-398, (1991).

11. Achiba, Y., Nakagawa, T., Matsui, Y., Suzuki, S., Shiromaru, H., Yamauchi, K., Nishiyama, K., Kainosho, M., Maruyama, Y. & Mitani, T. Visible, UV, and VUV Absorption Spectra of C_{60} Thin Films Grown by Molecular-Beam Epitaxy (MBE) Technique. *Chem Lett* **20**, 1233-1236, (1991).

12. Taylor, R. & Walton, D. R. M. The Chemistry of Fullerenes. *Nature* **363**, 685-693, (1993).

13. Haufler, R. E., Conceicao, J., Chibante, L. P. F., Chai, Y., Byrne, N. E., Flanagan, S., Haley, M. M., Obrien, S. C., Pan, C., Xiao, Z., Billups, W. E., Ciufolini, M. A., Hauge, R. H., Margrave, J. L., Wilson, L. J., Curl, R. F. & Smalley, R. E. Efficient Production of C60 (Buckminsterfullerene), C60h36, and the Solvated Buckide Ion. *J Phys Chem-Us* **94**, 8634-8636, (1990).

14. Chiang, L. Y., Swirczewski, J. W., Hsu, C. S., Chowdhury, S. K., Cameron, S. & Creegan, K. Multi-hydroxy Additions onto C60 Fullerene Molecules. *J. Chem. Soc. Chem. Commun.*, 1791-1793, (1992).

15. Guldi, D. M. & Prato, M. Excited-State Properties of C60 Fullerene Derivatives. *Acc. Chem. Res.* **33**, 695-703, (2000).

16. Arbogast, J. W., Darmanyan, A. P., Foote, C. S., Rubin, Y., Diederich, F. N., Alvarez, M. M., Anz, S. J. & Whetten, R. L. Photophysical Properties of C60. *J Phys Chem-Us* **95**, 11-12, (1991).

17. Ausman, K. D. & Weisman, R. B. Kinetics of Fullerene Triplet States. *Res. Chem. Intermed.* **1997**, 431-451, (1997).

18. Weisman, R. B. in *Optical and Electronic Properties of Fullerenes and Fullerene-Based Materials* (eds Joseph Sinar, Zeev Valvy Vardeny, & Zakya H. Kafafi) 84 (Marcel Dekker, Inc., 2000).

19. Andersson, T., Nilsson, K., Sundahl, M., Westman, G. & Wennerstrom, O. C-60 Embedded in Gamma-Cyclodextrin - a Water-Soluble Fullerene. *J Chem Soc Chem Comm*, 604-606, (1992).

20. Atwood, J. L., Koutsantonis, G. A. & Raston, C. L. Purification of C-60 and C-70 by Selective Complexation with Calixarenes. *Nature* **368**, 229-231, (1994).

21. Moussa, F., Trivin, F., Ceolin, R., Hadchouel, M., Sizaret, P. Y., Greugny, V., Fabre, C., Rassat, A. & Szwarc, H. Early effects of C-60 administration in Swiss mice: A preliminary account for in vivo C-60 toxicity. *Fullerene Sci Techn* **4**, 21-29, (1996).

22. Garaud, J. L., Janot, J. M., Miquel, G. & Seta, P. Photoinduced Electron-Transfer Properties of Porous Polymer Membranes Doped with the Fullerene C(60) Associated with Phospholipids. *J Membrane Sci* **91**, 259-264, (1994).

23. Hwang, K. C. & Mauzerall, D. Vectorial Electron-Transfer from an Interfacial Photoexcited Porphyrin to Ground-State C-60 and C-70 and from Ascorbate to Triplet C-60 and C-70 in a Lipid Bilayer. *J Am Chem Soc* **114**, 9705-9706, (1992).

24. Bensasson, R. V., Bienvenue, E., Dellinger, M., Leach, S. & Seta, P. C60 in Model Biological-Systems - a Visible-Uv Absorption Study of Solvent-Dependent Parameters and Solute Aggregation. *J Phys Chem-Us* **98**, 3492-3500, (1994).

25. Bakry, R., Vallant, R. M., Najam-ul-Haq, M., Rainer, M., Szabo, Z., Huck, C. W. & Bonn, G. K. Medicinal applications of fullerenes. *Int J Nanomedicine* **2**, 639-649, (2007).

26. Friedman, S. H., Decamp, D. L., Sijbesma, R. P., Srdanov, G., Wudl, F. & Kenyon, G. L. Inhibition of the Hiv-1 Protease by Fullerene Derivatives - Model-Building Studies and Experimental-Verification. *J Am Chem Soc* **115**, 6506-6509, (1993).

27. Sijbesma, R., Srdanov, G., Wudl, F., Castoro, J. A., Wilkins, C., Friedman, S. H., Decamp, D. L. & Kenyon, G. L. Synthesis of a Fullerene Derivative for the Inhibition of Hiv Enzymes. *J Am Chem Soc* **115**, 6510-6512, (1993).

28. Brettreich, M. & Hirsch, A. A highly water-soluble dendro[60]fullerene. *Tetrahedron Lett* **39**, 2731-2734, (1998).

29. Schuster, D. I., Wilson, S. R., Kirschner, A. N., Schinazi, R. F., Schlueter-Wirtz, S., Tharnish, P., Barnett, T., Ermolieff, J., Tang, J., Brettreich, M. & Hirsch, A. Evaluation of the Anti-HIV Potency of a Water-Soluble Dendrimeric Fullerene. *Proc. Electrochem. Soc.* **PV2000-9**, 267-270, (2000).

30. Marchesan, S., Da Ros, T., Spalluto, G., Balzarini, J. & Prato, M. Anti-HIV properties of cationic fullerene derivatives. *Bioorg Med Chem Lett* **15**, 3615-3618, (2005).

31. Bosi, S., Da Ros, T., Spalluto, G., Balzarini, J. & Prato, M. Synthesis and anti-HIV properties of new water-soluble bis-functionalized[60]fullerene derivatives. *Bioorg Med Chem Lett* **13**, 4437-4440, (2003).

32. Kotelnikova, R. A., Bogdanov, G. N., Frog, E. C., Kotelnikov, A. I., Shtolko, V. N., Romanova, V. S., Andreev, S. M., Kushch, A. A., Fedorova, N. E., Medzhidova, A. A. & Miller, G. G. Nanobionics of pharmacologically active derivatives of fullerene C-60. *J Nanopart Res* **5**, 561-566, (2003).

33. Kasermann, F. & Kempf, C. Photodynamic inactivation of enveloped viruses by buckminsterfullerene. *Antiviral Res* **34**, 65-70, (1997).

34. Zakharian, T. Y., Seryshev, A., Sitharaman, B., Gilbert, B. E., Knight, V. & Wilson, L. J. A fullerene-paclitaxel chemotherapeutic: Synthesis, characterization, and study of biological activity in tissue culture. *J Am Chem Soc* **127**, 12508-12509, (2005).

35. Krusic, P. J., Wasserman, E., Keizer, P. N., Morton, J. R. & Preston, K. F. Radical reactions of C60. *Science* **254**, 1183-1185, (1991).

36. Lin, A. M., Chyi, B. Y., Wang, S. D., Yu, H. H., Kanakamma, P. P., Luh, T. Y., Chou, C. K. & Ho, L. T. Carboxyfullerene prevents iron-induced oxidative stress in rat brain. *J Neurochem* **72**, 1634-1640, (1999).

37. Lin, A. M. Y., Fang, S. F., Lin, S. Z., Chou, C. K., Luh, T. Y. & Ho, L. T. Local carboxyfullerene protects cortical infarction in rat brain. *Neurosci Res* **43**, 317-321, (2002).

38. Chen, Y. W., Hwang, K. C., Yen, C. C. & Lai, Y. L. Fullerene derivatives protect against oxidative stress in RAW 264.7 cells and ischemia-reperfused lungs. *Am J Physiol Regul Integr Comp Physiol* **287**, R21-26, (2004).

39. Dugan, L. L., Turetsky, D. M., Du, C., Lobner, D., Wheeler, M., Almli, C. R., Shen, C. K., Luh, T. Y., Choi, D. W. & Lin, T. S. Carboxyfullerenes as neuroprotective agents. *Proc Natl Acad Sci U S A* **94**, 9434-9439, (1997).

40. Bisaglia, M., Natalini, B., Pellicciari, R., Straface, E., Malorni, W., Monti, D., Franceschi, C. & Schettini, G. C3-fullero-tris-methanodicarboxylic acid protects cerebellar granule cells from apoptosis. *J Neurochem* **74**, 1197-1204, (2000).

41. Huang, Y. L., Shen, C. K., Luh, T. Y., Yang, H. C., Hwang, K. C. & Chou, C. K. Blockage of apoptotic signaling of transforming growth factor-beta in human hepatoma cells by carboxyfullerene. *Eur J Biochem* **254**, 38-43, (1998).

42. Straface, E., Natalini, B., Monti, D., Franceschi, C., Schettini, G., Bisaglia, M., Fumelli, C., Pincelli, C., Pellicciari, R. & Malorni, W. C3-fullero-tris-methanodicarboxylic acid protects epithelial cells from radiation-induced anoikia by influencing cell adhesion ability. *Febs Lett* **454**, 335-340, (1999).

43. Yamakoshi, Y., Umezawa, N., Ryu, A., Arakane, K., Miyata, N., Goda, Y., Masumizu, T. & Nagano, T. Active oxygen species generated from photoexcited fullerene (C_{60}) as potential medicines: $O_2^{-\cdot}$ versus $^1O_2$. *J Am Chem Soc* **125**, 12803-12809, (2003).

44. An, Y. Z., Chen, C. H. B., Anderson, J. L., Sigman, D. S., Foote, C. S. & Rubin, Y. Sequence-specific modification of guanosine in DNA by a C-60-linked deoxyoligonucleotide: Evidence for a non-singlet oxygen mechanism. *Tetrahedron* **52**, 5179-5189, (1996).

45. Ikeda, A., Doi, Y., Hashizume, M., Kikuchi, J. & Konishi, T. An extremely effective DNA photocleavage utilizing functionalized liposomes with a fullerene-enriched lipid bilayer. *J Am Chem Soc* **129**, 4140-4141, (2007).

46. Tokuyama, H., Yamago, S., Nakamura, E., Shiraki, T. & Sugiura, Y. Photoinduced Biochemical-Activity of Fullerene Carboxylic-Acid. *J Am Chem Soc* **115**, 7918-7919, (1993).

47. Devasagayam, T. P. A., Kamat, J. P., Priyadarsini, K. I., Mohan, H. & Mittal, J. P. Oxidative damage induced by the fullerene C-60 on photosensitization in rat liver microsomes. *Chem-Biol Interact* **114**, 145-159, (1998).

48. Mohan, H., Kamat, J. P., Devasagayam, T. P. A. & Priyadarsini, K. I. Reactive oxygen species mediated membrane damage induced by fullerene derivatives and its possible biological implications. *Toxicology* **155**, 55-61, (2000).

49. Yang, X. L., Huang, C., Qiao, X. G., Yao, L., Zhao, D. X. & Tan, X. Photo-induced lipid peroxidation of erythrocyte membranes by a bis-methanophosphonate fullerene. *Toxicol in Vitro* **21**, 1493-1498, (2007).

50. Kasermann, F. & Kempf, C. Buckminsterfullerene and photodynamic inactivation of viruses. *Rev Med Virol* **8**, 143-151, (1998).

51. Hirayama, J., Abe, H., Kamo, N., Shinbo, T., Ohnishi-Yamada, Y., Kurosawa, S., Ikebuchi, K. & Sekiguchi, S. Photoinactivation of vesicular stomatitis virus with fullerene conjugated with methoxy polyethylene glycol amine. *Biol Pharm Bull* **22**, 1106-1109, (1999).

52. Lin, Y. L., Lei, H. Y., Wen, Y. Y., Luh, T. Y., Chou, C. K. & Liu, H. S. Light-independent inactivation of dengue-2 virus by carboxyfullerene C3 isomer. *Virology* **275**, 258-262, (2000).

53. Hamblin, M. R., Mroz, P., Tegos, G. P., Gali, H., Wharton, T. & Sarna, T. Photodynamic therapy with fullerenes. *Photoch Photobio Sci* **6**, 1139-1149, (2007).

54. Durantini, E. N., Spesia, M. B. & Milanesio, A. E. Synthesis, properties and photodynamic inactivation of Escherichia coli by novel cationic fullerene C(60) derivatives. *Eur J Med Chem* **43**, 853-861, (2008).

55. Prylutskyy, Y. L., Burlaka, A. P., Sidorik, Y. P., Prylutska, S. V., Matyshevska, O. P., Golub, O. A. & Scharff, P. Catalytic system of the reactive oxygen species on the C-60 fullerene basis. *Exp Oncol* **26**, 326-327, (2004).

56. Mroz, P., Pawlak, T., Satti, M., Lee, H., Wharton, T., Gali, H., Sarna, T. & Hamblin, M. R. Functionalized fullerenes mediate photodynamic killing of cancer cells: Type I versus Type II photochemical mechanism. *Free Radical Bio Med* **43**, 711 - 719, (2007).

57. Ikada, Y., Tabata, Y. & Murakami, Y. Photodynamic effect of polyethylene glycol-modified fullerene on tumor. *Jpn J Cancer Res* **88**, 1108-1116, (1997).

58. Liu, J., Ohta, S., Sonoda, A., Yamada, M., Yamamoto, M., Nitta, N., Murata, L. & Tabata, Y. Preparation of PEG-conjugated fullerene containing Gd(3+) ions for photodynamic therapy. *J. Controlled Release* **117**, 104, (2007).

59. Dresselhaus, M. S., Dresselhaus, G. & Saito, R. in *Nanotechnology* (ed Gregory Timp) (Springer-Verlag, 1999).

60. Murayama, H., Tomonoh, S., Alford, J. M. & Karpuk, M. E. Fullerene production in tons and more: From science to industry. *Fuller Nanotub Car N* **12**, 1-9, (2004).

61. Korobov, M. V. & Smith, A. L. in *Fullerenes: Chemistry, Physics, and Technology* (eds K. M. Kadish & R. S. Ruoff) 60 (John Wiley and Sons, Inc., 2000).

62. Andrievsky, G. V., Kosevich, M. V., Vovk, O. M., Shelkovsky, V. S. & Vashchenko, L. A. On the Production of an Aqueous Colloidal Solution of Fullerenes. *J Chem Soc Chem Comm*, 1281-1282, (1995).

63. Deguchi, S., Alargova, R. G. & Tsujii, K. Stable dispersions of fullerenes, C-60 and C-70, in water. Preparation and characterization. *Langmuir* **17**, 6013-6017, (2001).

64. Scrivens, W. A., Tour, J. M., Creek, K. E. & Pirisi, L. Synthesis of C-14-Labeled C-60, Its Suspension in Water, and Its Uptake by Human Keratinocytes. *J Am Chem Soc* **116**, 4517-4518, (1994).

65. Cheng, X., Kan, A. T. & Tomson, M. B. Naphthalene Adsorption and Desorption from Aqueous C60 Fullerene. *J Chem Eng Data* **49**, 675 - 683, (2004).

66. Brant, J. A., Labille, J., Bottero, J. Y. & Wiesner, M. R. Characterizing the impact of preparation method on fullerene cluster structure and chemistry. *Langmuir* **22**, 3878-3885, (2006).

67. Labille, J., Brant, J., Villieras, F., Pelletier, M., Thill, A., Masion, A., Wiesner, M., Rose, J. & Bottero, J. Y. Affinity of C-60 fullerenes with water. *Fuller Nanotub Car N* **14**, 307-314, (2006).

68. Hilburn, M. E., Murdianti, B. S., Maples, R. D., Williams, J. S., Damron, J. T., Kuriyavar, S. I. & Ausman, K. D. Synthesizing aqueous fullerene colloidal suspensions by new solvent-exchange methods. *Colloids and Surfaces A: Physicochemical and Engineering Aspects* **401**, 48-53, (2012).

69. Henry, T. B., Menn, F. M., Fleming, J. T., Wilgus, J., Compton, R. N. & Sayler, G. S. Attributing effects of aqueous C_{60} nano-aggregates to tetrahydrofuran decomposition products in larval zebrafish by assessment of gene expression *Environmental Health Perspective* **115**, 1059-1065, (2007).

70. Oberdorster, E. Manufactured nanomaterials (Fullerenes, C-60) induce oxidative stress in the brain of juvenile largemouth bass. *Environ Health Persp* **112**, 1058-1062, (2004).

71. Sayes, C. M., Fortner, J. D., Guo, W., Lyon, D., Boyd, A. M., Ausman, K. D., Tao, Y. J., Sitharaman, B., Wilson, L. J., Hughes, J. B., West, J. L. & Colvin, V. L. The differential cytotoxicity of water-soluble fullerenes. *Nano Lett* **4**, 1881-1887, (2004).

72. Dhawan, A., Taurozzi, J. S., Pandey, A. K., Shan, W., Miller, S. M., Hashsham, S. A. & Tarabara, V. V. Stable colloidal dispersions of C60 fullerenes in water: evidence for genotoxicity. *Environ Sci Technol* **40**, 7394-7401, (2006).

73. Lyon, D. Y. & Alvarez, P. J. Fullerene water suspension (nC60) exerts antibacterial effects via ROS-independent protein oxidation. *Environ Sci Technol* **42**, 8127-8132, (2008).

74. Sayes, C. M., Gobin, A. M., Ausman, K. D., Mendez, J., West, J. L. & Colvin, V. L. Nano-C-60 cytotoxicity is due to lipid peroxidation. *Biomaterials* **26**, 7587-7595, (2005).

75. Zhu, S. Q., Oberdorster, E. & Haasch, M. L. Toxicity of an engineered nanoparticle (fullerene, C-60) in two aquatic species, Daphnia and fathead minnow. *Mar Environ Res* **62**, S5-S9, (2006).

76. Zhu, X., Zhu, L., Lang, Y. & Chen, Y. Oxidative stress and growth inhibition in the freshwater fish Carassius auratus induced by chronic exposure to sublethal fullerene aggregates. *Environ Toxicol Chem* **27**, 1979-1985, (2008).

77. Andrievsky, G., Klochkov, V. & Derevyanchenko, L. Is the C-60 fullerene molecule toxic?! *Fuller Nanotub Car N* **13**, 363-376, (2005).

78. Gharbi, N., Pressac, M., Hadchouel, M., Szwarc, H., Wilson, S. R. & Moussa, F. [60]fullerene is a powerful antioxidant in vivo with no acute or subacute toxicity. *Nano Lett* **5**, 2578-2585, (2005).

79. Levi, N., Hantgan, R. R., Lively, M. O., Carroll, D. L. & Prasad, G. L. C60-fullerenes: detection of intracellular photoluminescence and lack of cytotoxic effects. *J Nanobiotechnology* **4**, 14, (2006).

80. Shinohara, N., Matsumoto, T., Gamo, M., Miyauchi, A., Endo, S., Yonezawa, Y. & Nakanishi, J. Is lipid peroxidation induced by the aqueous suspension of fullerene C60 nanoparticles in the brains of Cyprinus carpio? *Environ Sci Technol* **43**, 948-953, (2009).

81. Henry, T. B., Menn, F. M., Fleming, J. T., Wilgus, J., Compton, R. N. & Sayler, G. S. Attributing effects of aqueous C60 nano-aggregates to tetrahydrofuran

decomposition products in larval zebrafish by assessment of gene expression. *Environ Health Perspect* **115**, 1059-1065, (2007).

82. Spohn, P., Hirsch, C., Hasler, F., Bruinink, A., Krug, H. F. & Wick, P. C-60 fullerene: A powerful antioxidant or a damaging agent? The importance of an in-depth material characterization prior to toxicity assays. *Environ Pollut* **157**, 1134-1139, (2009).

CHAPTER III

C_{60} OXIDE AS A KEY COMPONENT OF AQUEOUS C_{60} COLLOIDAL SUSPENSIONS

Introduction

The reported methods to disperse C_{60} in water as a colloidal suspension without deliberate functionalization of the molecule include dissolution in an organic solvent followed by mixing with water and driving off the organic solvent by ultrasonication (also known as sonication method), [1-3] organic solvent exchange (also known as the TTA, HIPA, HEA or THF method),[2,4,5] and simple long-time stirring of C_{60} powder in water (also known as the aqua method).[2,6]

The synthesis of nano-C_{60} by various methods described above occurs under ambient atmosphere. In this chapter, discussion of the formation of stable aqueous C_{60} aggregates will be focused on the AQU/*n*C_{60} method. This method is of particular interest for several reasons: (1) AQU/*n*C_{60} method is likely the most environmentally relevant form of *n*C_{60}, (2) there are major unanswered questions about why this colloid is stable in water in the first place, and (3) the oxidation studies (discussed in the next

chapter) show that there is still some oxidation occurring even in samples that do not include tetrahydrofuran. Therefore, it is important to understand the structure and chemistry of samples that have the fewest additional materials such as left-over organic solvents in the system. For this study, AQU/*n*C_{60} method was prepared under controlled atmospheric conditions. Under inert atmospheric conditions, the formation of colloidal C_{60} is significantly inhibited as compared to the sample prepared under ambient conditions. Initial studies in our lab also showed that the C_{60} epoxide derivative was formed during the synthesis of *n*C_{60} under ambient atmosphere.

For the purpose of this study, samples of AQU/*n*C_{60} were prepared, using pristine (P) and oxide enriched (O) C_{60} solids as starting materials, each prepared under inert (I) and ambient (A) atmospheres. The *n*C_{60} samples formed for this study are characterized at multiple stirring times for their concentrations, derivative content, and particle size.

Experimental

C_{60} with 99.9% purity was purchased from MER Coorporation, Tucson, AZ. Ultrapure water used throughout the experiments was provided from Direct-Q 3 UV System (Millipore, Billerica, MA) with resistivity greater than 18 MΩ·cm. Anhydrous Na_2SO_4 was purchased from Fisher Scientific, Fair Land, NJ. HPLC Grade toluene was purchased from Pharmco, Brookefield, CT. Ozone (O_3) gas was generated with an Ozone Servicesozonator (Yanco Industries Ltd.). Gases were purchased from Stillwater Steel and Welding Supply, Stillwater, OK.

Preparation of $C_{60}O$-enriched solid

$C_{60}O$-enriched solid was prepared by a method similar to that reported by Chibante *et al.*[7] Briefly 50 mg of C_{60} solid was dissolved in 250 mL of toluene and allowed to stir overnight in a round bottom flask. O_3-enriched O_2 was generated by the ozonator in a 0.2 L/min. stream of O_2. This stream was then diluted 4:1 by N_2 to give a total flow-rate of 1.0 L/min. A fraction of this gas mixture was bubbled through the solution at room temperature at a rate of 0.2 L/min for 30 seconds. The manufacturer-estimated ozone output under the experimental conditions after dilution is 2.28 mg/min, and thus approximately 1.14 mg O_3 should have passed through the sample. The samples were kept in the dark and allowed to stand for 1 hour at room temperature. An aliquot (1 mL) was filtered through a 0.02-µm-Whatman®Anotop™ filter (Fisher Scientific, Suwanee, GA) for HPLC analysis. Toluene was removed from the $C_{60}O$-enriched sample by rotary evaporation to dryness (Heidolph HB control rotavap) at 75 mbar pressure and temperature of 45^{o}C. The solids were air dried for several days before further use.

Preparation of aqu/C_{60} aggregates

Samples were prepared under ambient and inert atmosphere conditions and using pristine C_{60} (99.9%) and $C_{60}O$-enriched sample as starting materials, as described below.

- Sample P-A: pristine C_{60} solids mixed under ambient air
- Sample P-I: pristine C_{60} solid mixed under a nitrogen atmosphere
- Sample O-A: $C_{60}O$-enriched solids mixed under ambient air
- Sample O-I: $C_{60}O$-enriched solids mixed under a nitrogen atmosphere

Aqu/n-C_{60} samples were prepared by a modification of published methods.[2,6,8] Approximately 50 mg of pristine C_{60} or $C_{60}O$-enriched solids were added to separate 500 mL round-bottomed flasks. 100 mL of ultrapure water was added to each container. For samples prepared under a nitrogen atmosphere, the flasks were sealed and samples and headspaces were purged by bubbling nitrogen gas for 30 minutes to remove dissolved oxygen. All samples were then stirred with magnetic stirrers for seven days. Aliquots from each sample were obtained at 1, 24, 72 and 168 hours after stirring was started. These aliquots were filtered through a 0.45-μm-MCE filter (Fisher Scientific, Denver, CO) to remove any undispersed material. Fullerene aggregates produced by this synthesis method (aqu/n-C_{60}) were characterized for particle size distribution by dynamic light scattering, for quantitative concentration determination by UV-Visible spectroscopy, and for C_{60} derivatives by HPLC.

Characterization

Light Scattering Measurements

The size distribution for fullerene aggregates was performed by dynamic light scattering (DLS) measurement at 25^{o}C on a DAWN® HELEOS™ 243-HHC (Wyatt Technology Corp.) equipped with Ga-As laser (60 mW) operating at a wavelength of 658.0 nm. The measurements were performed at a 99^{o} scattering angle (Detector #12). To obtain the hydrodynamic radius of the fullerene aggregates, the autocorrelation function of the scattered light intensity was analyzed by a regularization analysis. In this analysis, the autocorrelation function is fitted with a proprietary non-negative least squares algorithm,

known as regularization algorithm, where the algorithm makes no prior assumptions about the shape or form of the size distribution. Static light scattering intensity was also recorded for the samples at 90° (Detector #11) as a more sensitive, but less-quantitative indication of concentration than the extraction procedure described below.

Quantitative Concentration Analysis of C_{60}

The concentration of C_{60} aggregates was determined using a liquid-liquid extraction technique similar to that reported by Deguchi, *et al.*[1] Briefly 1 mL of *n*C_{60} samples, 2 mL of 10% (W/V) $NaNO_3$ and 3 mL toluene (HPLC Grade) were combined in a small vial, capped and sonicated in an ultrasound bath for 10 minutes. The mixture was allowed to stand for at least 2 hours or until the toluene and aqueous layers separated. Each layer was analyzed separately using a Cary 5000 UV-Vis Spectrophotometer from Varian, scanning from 300 – 800 nm. Toluene and nanopure water were used as backgrounds for the toluene and aqueous layers respectively. The concentration of C_{60} in the toluene layer was determined by fitting the measured spectrum to calibrated reference spectra. A lack of absorbance in the aqueous layer was taken to indicate complete extraction.

HPLC analysis for C_{60} derivatives

Extraction of C_{60} and its derivatives from aqu/n-C_{60} was performed by adding 2 mL of 10% (W/V) $NaNO_3$ and 1.5 mL toluene (HPLC Grade) to 6 mL of aqu/n-C_{60}. The mixture was stirred overnight and the toluene layer was separated from the mixture. The aqueous layer from the extraction was analyzed using UV-Vis spectrophotometer Cary 5000 from Varian to verify that all C_{60} and its derivatives were extracted into toluene. The

toluene layer was dried using anhydrous Na_2SO_4 and filtered through a 0.02-µm-Whatman®Anotop™ filter (Fisher Scientific, Suwanee, GA). Toluene filtrates were analyzed on an HPLC system from Varian consisting of a 210 ProStar Solvent Delivery Module, a Rheodyne 7725i injection valve with an injection volume of 20 µL, and a 355 ProStar Photo Diode Array detector with deuterium (UV) and quartz iodide (visible) lamp source, all operated through Galaxie™ Chromatography Workstation. Spectra were collected at all retention times from 300 to 450 nm. The chromatograms presented in this work were recorded at 336 nm, where the C_{60} spectrum has a local maximum. The column used was a NacalaiTesque "CosmosilBuckyprep", Waters type, 4.6 x 250 mm packed column, protected by a NacalaiTesque "CosmosilBuckyprep", Waters type, 4.6 x 10 mm guard column. HPLC Grade toluene was used as the mobile phase with a flow rate of 1 mL/min.

Result and Discussions

Ambient air condition is required for the formation of AQU/*n*C_{60}

The synthesis of *n*C_{60} using vigorous mixing of C_{60} solid in water (AQU/*n*C_{60}) typically requires weeks to prepare. Under ambient conditions similar to previously reported syntheses of AQU/*n*C_{60},[2,6,8] the formation of brownish suspensions was observed after one week of vigorous stirring, and with longer stirring time, the color intensity of the brownish suspensions deepens. In a parallel experiment of sample preparation under inert atmosphere, the brownish suspensions were not observed even after 3 weeks as shown in Figure 3.1. Most of the black solid material formed a thin black film on the water surface.

This result indicates that the synthesis of AQU/*n*C_{60} requires some components present in ambient air.

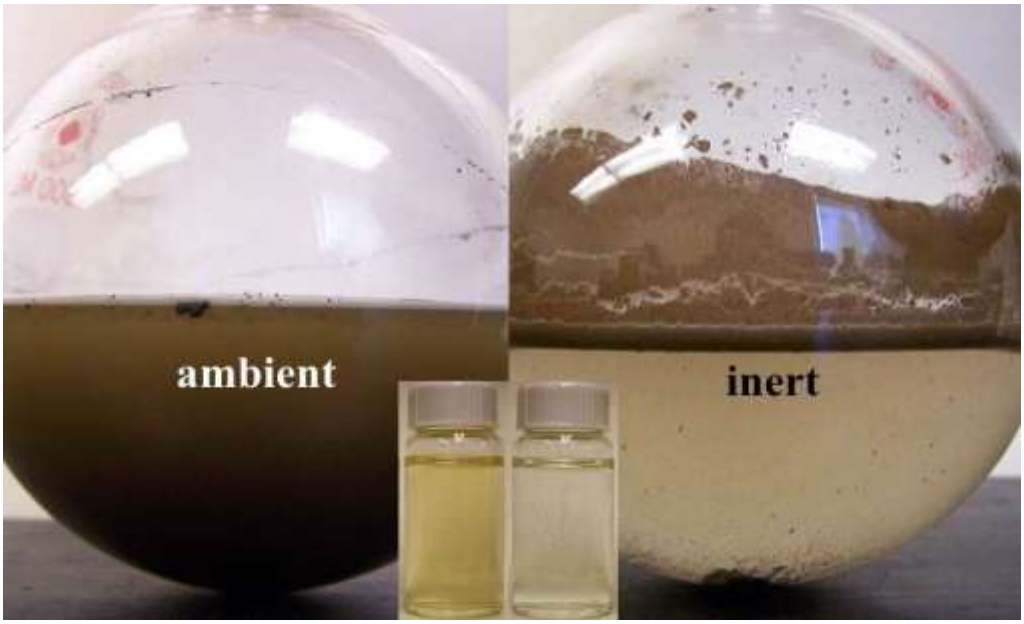

Figure 3.1 AQU/*n*C_{60} prepared under ambient (left) and inert (right) atmosphere after 3 weeks of vigorous stirring. The main figure and inset show the samples before and after filtration, respectively.

$C_{60}O$ and the formation of AQU/*n*C_{60}

In the HPLC analysis of C_{60} and its derivatives, aliquots to be analyzed were not extracted into toluene under sonication to avoid degradation of the derivatives. Extraction method for HPLC analysis by overnight stirring of a mixture of AQU/*n*C_{60} suspensions, 10% $NaNO_3$ and toluene was performed to extract the C_{60} and any C_{60} derivatives that may be present into toluene. After extraction, the water layer was analyzed using UV-visible spectroscopy to verify the absence of C_{60}'s characteristic absorption spectrum. In water, C_{60} has broader and less intense peaks in the UV region, as compared to the peaks

in toluene. The three strong absorption peaks of C_{60} in the UV region are also shifted to the longer wavelength than the peaks in toluene. In the visible region, the spectra of *n*C_{60} showed more significant difference as expected from the color change of the solution (purple in toluene and yellow in water). As can be seen in Figure 3.2, the sharp peak at 405 nm completely disappears, and a new broad absorption peak between 420 and 520 nm appears. This broad peak closely resembles that of a solid thin film.[9] After extraction, the absence of C_{60} broad absorption peaks at 218, 275, and 359 nm from the water layer (Figure 3.2) indicates a complete extraction of C_{60} into toluene layer.[1] High absorbance observed below 400 nm after extraction of *n*C_{60} is due to the absorbance by the salt used (*i.e.*, sodium nitrate).

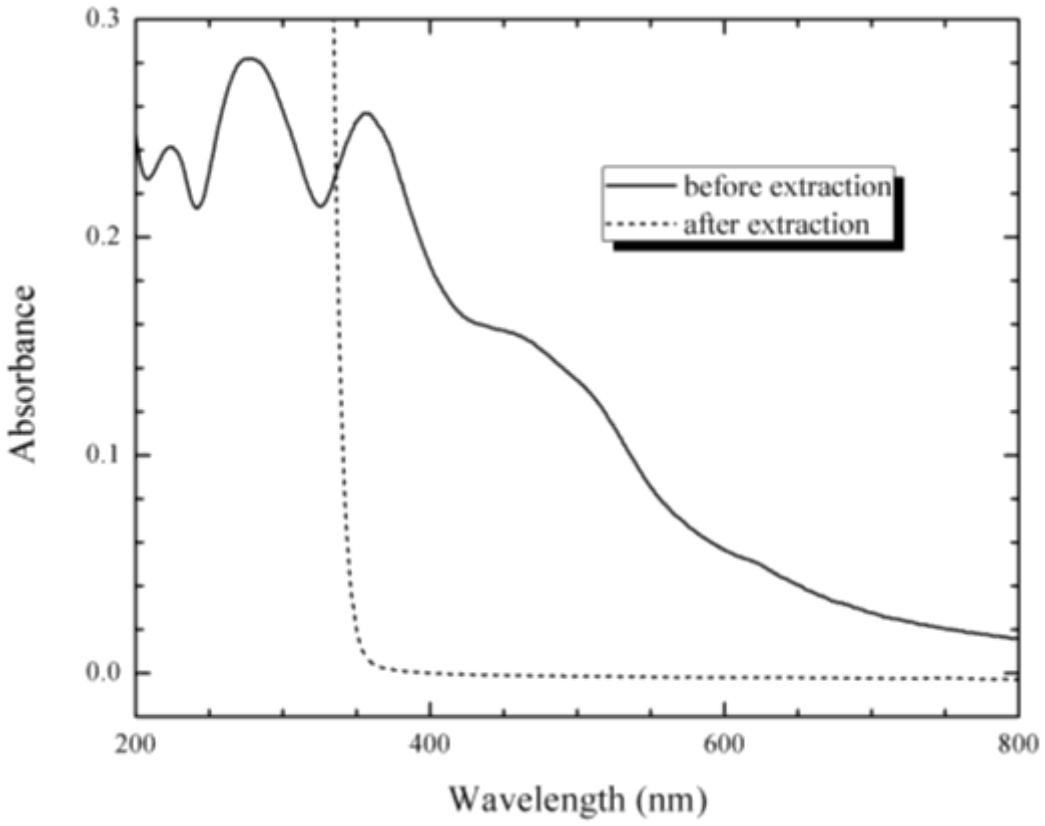

Figure 3.2 UV-visible spectrum of AQU/*n*C_{60} before and after extraction into toluene.

HPLC analysis of the toluene layer from the extraction of ambient-condition sample revealed a primary peak at retention time approximately 9 min as shown in Figure 3.3. This peak has a visible absorption maximum at 336 nm as shown in Figure 3.3, matching with the expected visible absorption for C_{60} in toluene.[10] A small peak at retention time approximately 10 min was observed immediately to follow after the primary peak. From the Figure 3.4, it can be seen that this peak has a visible absorption maximum at 328 nm, and a smaller absorption at 246 nm, matching in the absorption spectrum of [6,6]-closed epoxide $C_{60}O$.[7,11,12]

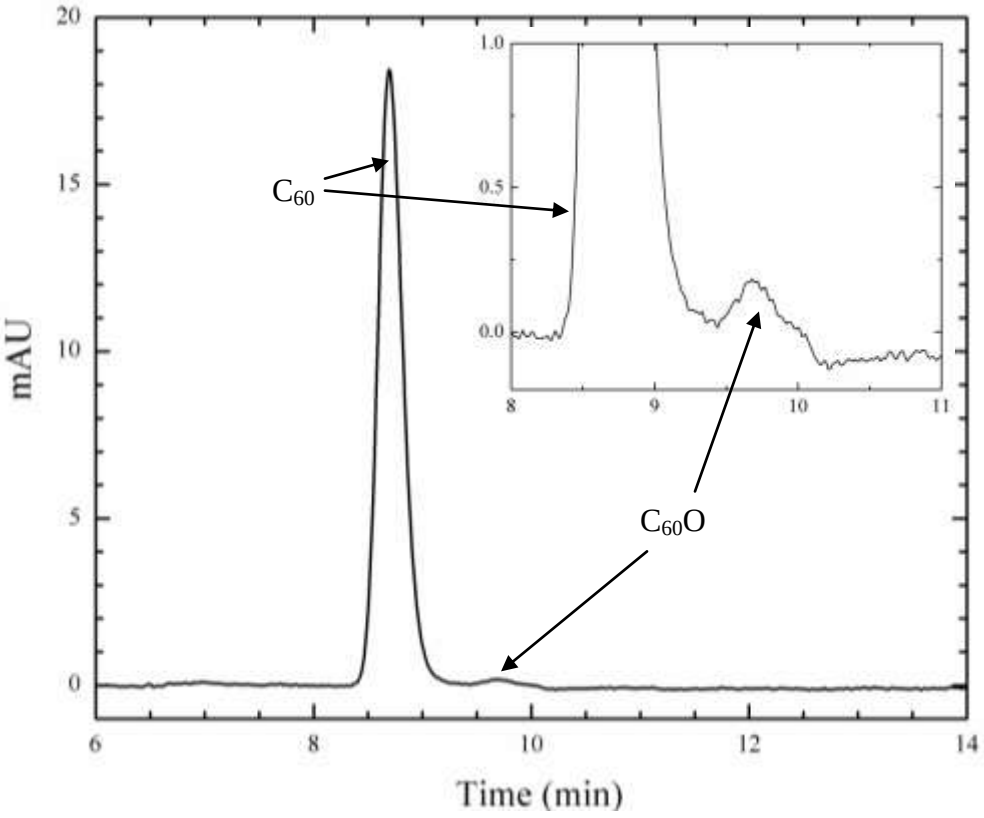

Figure 3.3 HPLC chromatogram at 336 nm from extraction of AQU/*n*C_{60} reveals the formation of $C_{60}O$.

As explained in Chapter II, there are two isomers of $C_{60}O$: [6,6]-closed epoxide and [5,6]-open oxidoannulene (Figure 2.3). Both isomers can be obtained through ozonolysis of C_{60} solution in toluene, which immediately forms an ozonide ($C_{60}O_3$). This ozonide is unstable and easily decays into $C_{60}O$ through thermolysis or photolysis pathways to form [6,6]-closed epoxide or [5,6]-open oxidoannulene, respectively, as shown in Figure 2.3.[12] These two isomers have an overlap retention time, however, the absorption spectrum of the two are clearly different. The [5,6]-open isomer has a visible absorption maximum at 336 nm, and lacking the feature near 426 nm, while the [6,6]-closed epoxide has a visible absorption maximum at 328 nm.

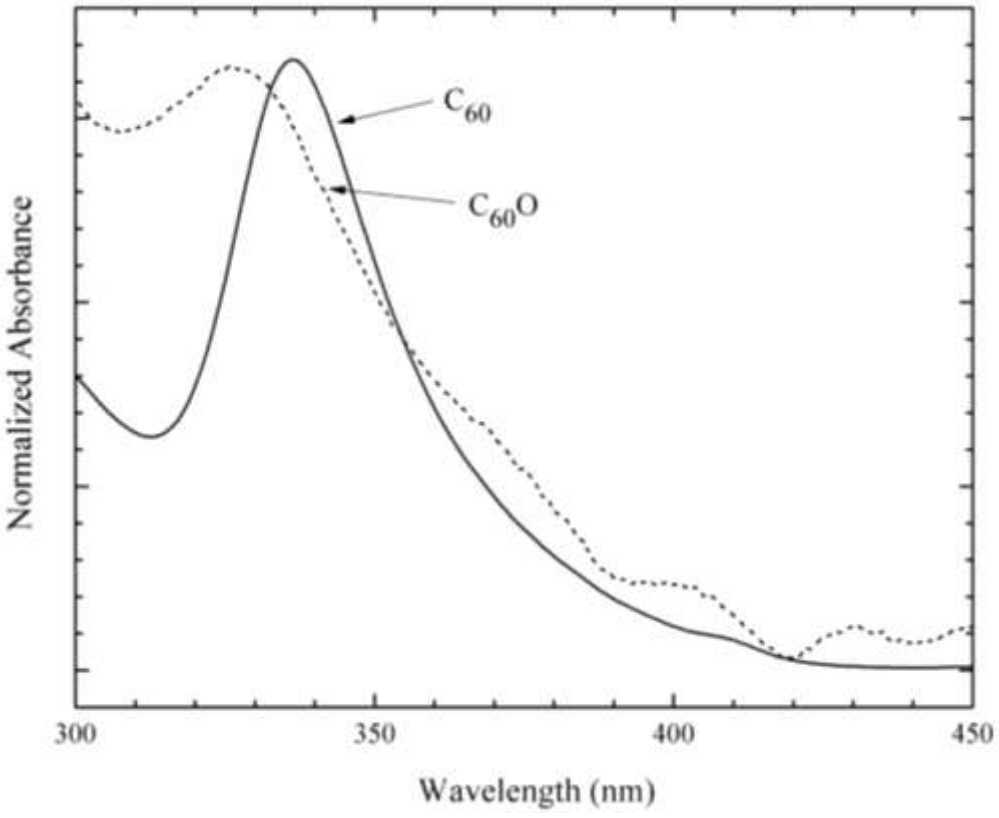

Figure 3.4 Absorption spectra measured by the HPLC's photodiode array absorption spectrometer for the C_{60} (solid line) and $C_{60}O$ (dotted line) peaks in a chromatogram of extracted aqu/*n*C_{60} produced under ambient conditions.

The absorption spectrum of the fullerene epoxide is clearly different from that of several other candidates for the identity of this component of the chromatogram, including the [5,6]-open isomer of $C_{60}O$ (λ_{max} = 336 nm and lacking the feature near 424 nm)[12] and the fullerols $C_{60}(OH)_{2-36}$ (λ_{max} = 320 nm for n=2, λ_{max} = 266 nm for n=36; intermediate values of n typically have intermediate absorption maxima).[13,14] From the observations on HPLC retention time, the small peak at 10 min retention time is matching with the one observed in deliberately-$C_{60}O$-enriched sample. Thus, there are several important points that can be highlighted. The first is the matching of both this UV-visible spectrum and that of the enriched sample to that reported for $C_{60}O$.The second is the observation of the HPLC retention time at 10 min between *n*C_{60} sample and the deliberately-$C_{60}O$-enriched sample, where both shows matching retention time for the observed $C_{60}O$. The third is the dependence of the colloid formation on the presence of atmospheric ozone (as discussed below), and the known mechanism for conversion of ozonated C_{60} to the C_{60} epoxide.[15] Because of these reasons, it is reasonable to conclude that the peak observed at retention time approximately 10 min is the epoxide form of C_{60}.

Using known extinction coefficients of $C_{60}O$ and C_{60} at 328 nm, the percentage of $C_{60}O$ in the ambient condition sample was able to be determined. From the 328 nm chromatogram, the ambient condition AQU/*n*C_{60} sample contained 1.72% $C_{60}O$ in quantities. This value is significantly in excess of that present in the original C_{60} (0.21%), which was also determined by HPLC analysis.

In order to demonstrate that the presence of the [6,6]-closed epoxide isomer of $C_{60}O$ was sufficient to allow the formation of AQU/*n*C_{60} in the absence of air, a sample of C_{60} enriched with the epoxide derivatives ($C_{60}O$) was used as an alternate starting

material in the synthesis. As expected, ozonation of C_{60} in toluene solution by the procedure given above resulted in a color change from purple to reddish purple. HPLC analysis of the enriched sample gave the expected primary peak for C_{60} at approximately 9 min, the expected enhanced secondary peak for $C_{60}O$ at approximately 10 min, and a clear indication of a small amount of higher oxides to follow at longer retention time as shown in Figure 3.5. The UV-visible spectra of the first and second HPLC peaks matched with the reported UV-visible spectra for C_{60} and $C_{60}O$ as shown in Figure 3.6, where C_{60} has a visible absorption maximum at 336 nm followed by a small peak at 405 nm and $C_{60}O$ has a visible absorption maximum at 328 nm followed by a characteristic peak at around 426 nm.[7,11,12] The percentage of $C_{60}O$ in this enriched sample was again determined using known extinction coefficients of $C_{60}O$ and C_{60} at 328 nm. The $C_{60}O$-enriched sample contained approximately 10% $C_{60}O$.

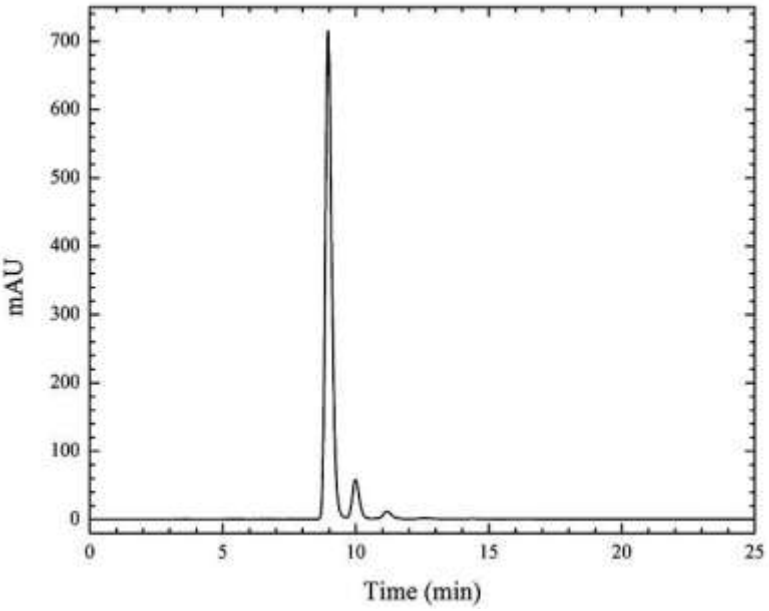

Figure 3.5. HPLC chromatogram of $C_{60}O$ enriched solids in toluene at 336 nm wavelength.

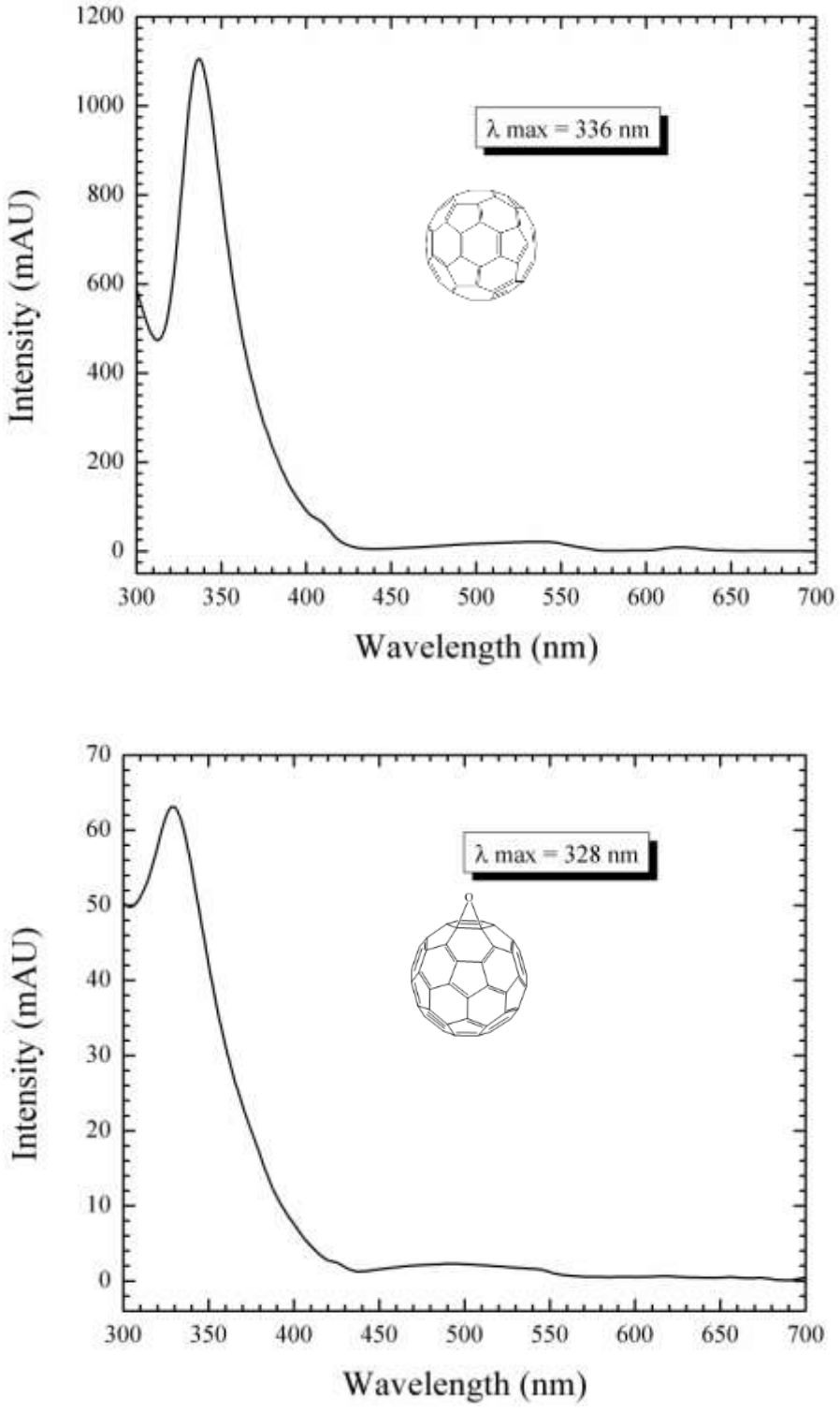

Figure 3.6. UV-visible spectrum for C_{60} (top) and $C_{60}O$ (bottom) in toluene, showing a peak maximum at 336 nm and 328 nm, respectively.

AQU/*n*C_{60} samples using pristine C_{60} and the $C_{60}O$-enriched solid were prepared as starting materials under both ambient and nitrogen atmospheres. Aliquots for detailed analysis from all four samples were removed and filtered at 1, 24, 72, and 168 h (1 week) after stirring was begun.

The formation of AQU/*n*C_{60} was observable by light scattering in both samples O-A and O-I after only one hour of stirring, whereas the aggregates formation was not observable for samples P-A and P-I. The resulting hydrodynamic radii for these two samples (O-A and O-I) were 139 and 81.3 nm respectively. After 24 h of stirring, samples O-A and O-I gave slightly brownish-colored suspensions after filtration, while samples P-A and P-I remained clear after the same time period (Figure 3.7). In previous preparations of AQU/*n*C_{60} in our laboratory, the brownish suspensions were not visually apparent until approximately 1 week of vigorous stirring under ambient conditions. The P-A sample gave slightly brownish-colored suspension after filtration after 1 week vigorous stirring, while P-I sample remained clear after the same time period.

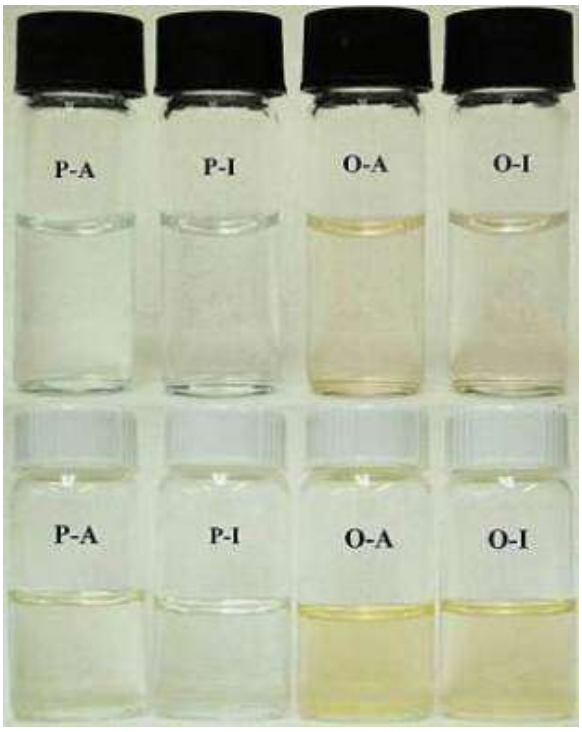

Figure 3.7. AQU/*n*C_{60} samples prepared using pristine C_{60} and C_{60}O-enriched sample (designated P and O, respectively). Aliquots shown were obtained after 24 h (top) and 168 h (bottom) mixing in water under ambient and inert conditions (designated A and I, respectively).

Sample concentrations were determined by extraction into toluene under bath sonication. Concentration results for each sample are summarized in Table 1. For P-A and P-I samples that have no detectable fullerene in the toluene extract have been left blank. All samples showed an increase in sample concentration with increased stirring time. Fullerene concentrations in the toluene extracts for samples P-A and P-I were not measurable until the 168 h aliquots, whereas both samples O-A and O-I were barely detectable by extraction after only one hour and easily detectable after 24 h. All samples were also examined by static light scattering to detect particles below the extraction

method's detection limit. Particle size as determined by dynamic light scattering are summarized in Table 2. The ambient atmosphere samples typically showed significantly greater nC$_{60}$ formation than the corresponding inert atmosphere samples.

Table 3. 1. Fullerene concentrations (ppm) for AQU/nC$_{60}$ samples as determined by extraction. The table entries are gray-scale-coded to static light scattering intensity.

	Stirring time (hours)			
Sample	1	24	72	168
P-A				0.41
P-I				0.11
O-A	0.12	0.77	0.85	1.11
O-I	0.02	0.22	0.89	0.88

Key: Light scattering detector voltage (V)

< 0.09	0.10–0.49	0.5–0.9	1.0–2.4	2.5–4.9	5.0–9.9	> 10.0

Table 3. 2. Mean hydrodynamic radii (nm) as determined by DLS for all aliquots.

	Stirring time (hours)			
Sample	1	24	72	168
P-A	N/A	105 ± 11.9	93.4 ± 15.7	87.4 ± 8.1
P-I	N/A	115 ± 21.6	84.9 ± 12.3	70.9 ± 6.8
O-A	139 ± 13	75.8 ± 3.1	76.4 ± 10.2	94.7 ± 6.9
O-I	81.3 ± 5.9	113 ± 6.7	69.9 ± 10.3	75.5 ± 5.1

HPLC analysis of the toluene extraction layer of samples O-A and O-I after 1 hour stirring gave a small peak (with the intensity approximately 1 mAU) at a retention time of 9 min. This peak's UV-visible spectrum had a local maximum at 336 nm, the characteristic absorbance for C_{60} in toluene. The same C_{60} peak was not observed in samples P-A and P-I C_{60} after one hour stirring. This observation is consistent with the lack of measurable fullerene content in the corresponding sonicated extracts. No $C_{60}O$ peak was observed due to the overall low concentrations of these aliquots.

After 24 h stirring, the intensity of C_{60} peak for samples O-A and O-I increased by 10 and 4 times over the corresponding peaks in the 1 h stirring aliquots, respectively, and the peak for $C_{60}O$ at 10 min retention time became apparent. For samples prepared using pristine C_{60}, a small peak (with a peak intensity of approximately 1 mAU) at 9 min retention time was observed in sample P-A after 24 h stirring, but not in sample P-I.

After 72 h stirring, the intensity of sample P-A's 9 min peak was double that of the comparable sample stirred for 24 h. The overall concentration of this aliquot was still too low to expect to observe a measurable $C_{60}O$ peak in the chromatogram. The intensity of the C_{60} peaks in samples O-A and O-I also increased, but there were still no measurable peaks in the chromatogram for sample P-I. These results agree with the visual changes observed in the four samples.

HPLC profiles for the four samples after 168 h of stirring are shown in Figure 3.8. The main C_{60} peak at 9 min retention time is observable for all of these aliquots. Not surprisingly, the 10 min retention time $C_{60}O$ peaks are easily visible in samples O-A and O-I, but it is also visible, though small, in sample P-A. The main C_{60} peak at a retention

time of 9 min was also observed in sample P-I. As discussed below, we believe that this small formation of $n$$C_{60}$ in this sample may be caused by the original 0.21% of $C_{60}O$ present in the starting material. The oxide-enriched colloidal samples O-A and O-I have $C_{60}O$ contents that are largely unchanged relative to the starting material (10.3% in the original material, 10.6% for O-A and 10.0% for O-I). This is not surprising given the smaller contribution of atmospheric ozone to colloid formation that is necessary in the oxide-enriched samples, and the lower degree of molecular mobility required during formation of the colloid particles under conditions with higher degrees of oxide content (discussed below).

These results show that (a) some component of the ambient atmosphere is required to form AQU/$n$$C_{60}$, (b) there is a significant difference between the fullerenes in the resulting $n$$C_{60}$ and the original fullerene sample is the enhancement of a small but measurable amount of the [6,6]-closed epoxide isomer of $C_{60}O$, and (c) by deliberately enriching the $C_{60}O$ content of the source fullerenes, it is sufficient to induce the formation of $n$$C_{60}$ even in the absence of contact with the ambient atmosphere. Based on these observations, we therefore propose that $C_{60}O$ is the key component of AQU/$n$$C_{60}$ that stabilizes the colloidal particles in water.

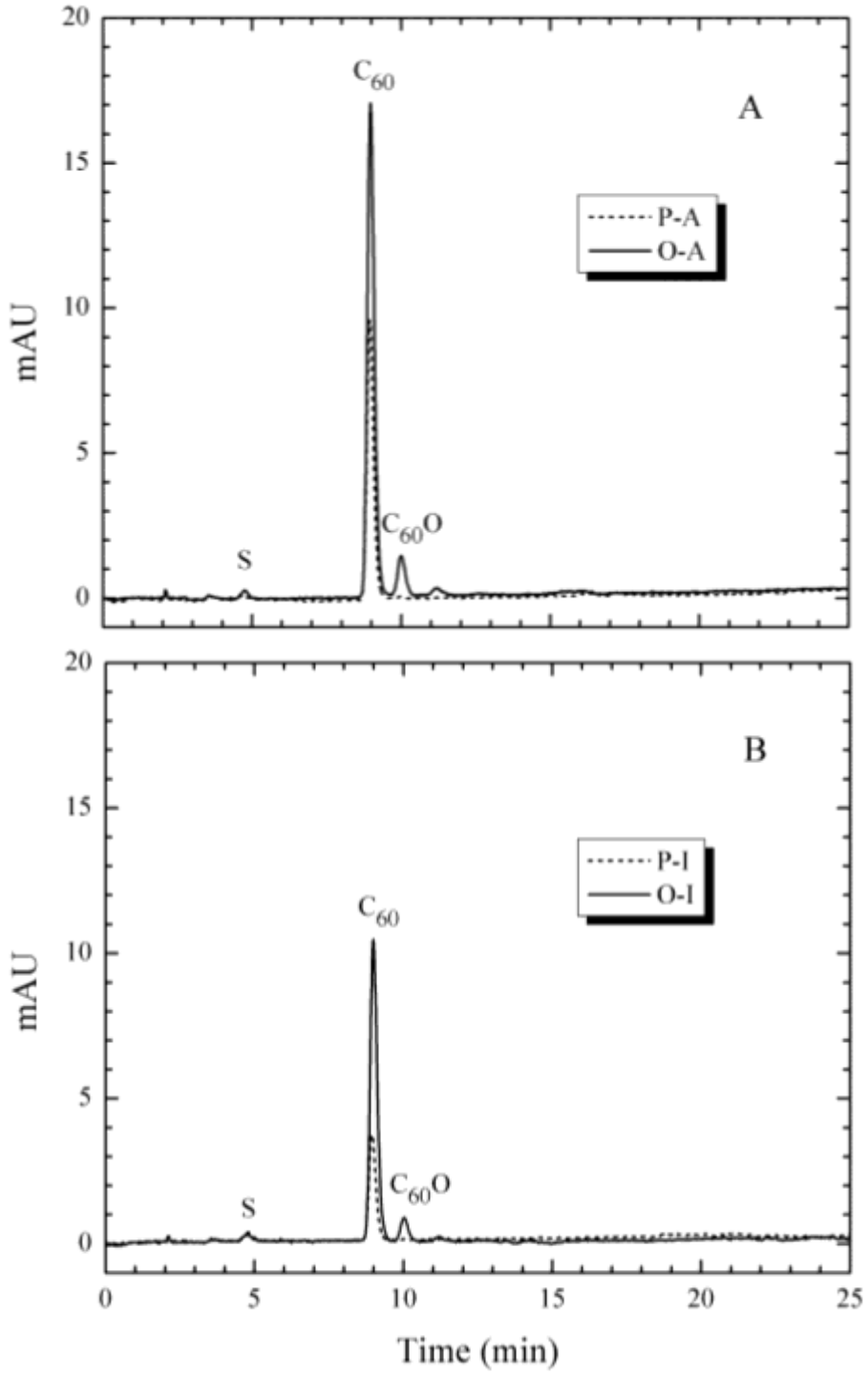

Figure 3.8. HPLC chromatogram at 336 nm of extracted AQU/*n*C_{60} samples under ambient (A) and inert (B) conditions into toluene after 168 h stirring in water. S = solvent peak.

Due to the cage structure of the fullerenes, the epoxide-form of $C_{60}O$ is unique among epoxides where the epoxide carbons are completely inaccessible to backside nucleophilic attack, and thus the molecule is relatively stable under environmental conditions. On the other hand, the epoxide functionality can act as a hydrogen-bond acceptor, thus somewhat stabilizing the epoxide portion of $C_{60}O$ in water. If we were to imagine an nC_{60} colloidal particle as a 100 nm diameter sphere, it would contain approximately 7.4×10^5 molecules, yet only 3.14×10^4 of them would be on the surface (this calculation assumes a face-centered cubic crystal structure for C_{60} with a unit cell edge of 1.417 nm,[16] and ignores the possibility of solvates). Thus a conversion of only 4.2% of the fullerene molecules to the epoxide form would be sufficient to completely cover the surface of the particle, thereby presenting a hydrophilic interface to the surrounding water. Given that the experimental $C_{60}O$ content of our original pristine sample is approximately 41% of this value, it appears that a sub-monolayer coverage is still sufficient to suspend the particles. Figure 3.9 depicts this level of derivatization. The red dots represent the oxygen atoms, while the C_{60} molecule is colored dark gray. The diameter of the particle is roughly 30 nm, and is shown in the FCC packing of a C_{60} crystal.

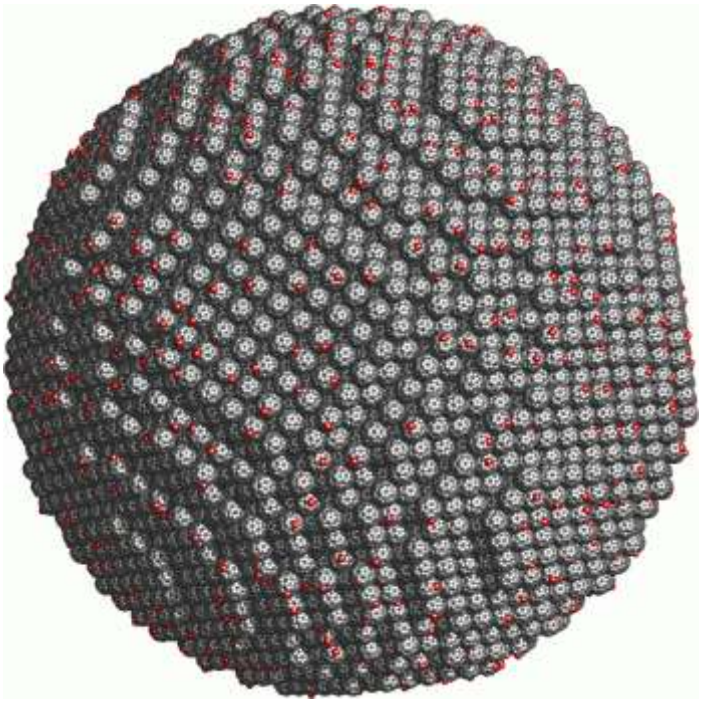

Figure 3.9. An illustration depicting an approximately 30 nm diameter colloidal particle where 41% of the surface fullerenes as C_{60}-oxide.

$C_{60}O$ formation by reaction with ambient ozone

A question that remains concerning this work is the origin of the $C_{60}O$ that is formed during an ambient atmosphere synthesis of AQU/*n*C_{60}. The photoactive nature of C_{60} is well-known, where the lowest triplet state of C_{60} has a tendency to undergo energy transfer with the molecular oxygen to form oxygen's excited singlet state.[17,18] Due to this property, it is tempting to relate the formation of $C_{60}O$ during the synthesis of AQU/*n*C_{60} to photoactivation of atmospheric and/or dissolved oxygen. This is unlikely to be the correct explanation, however, for three complementary reasons. First, although the photochemical oxidation of C_{60} to $C_{60}O$ has been reported,[11] that synthesis used 18 hours of high-intensity irradiation of an oxygenated benzene solution in an immersion well, conditions that are extreme compared to the ambient synthesis of AQU/*n*C_{60}. Second, in

the control studies performed on the synthesis of AQU/$n$$C_{60}$ in dark vs. ambient light conditions, no measurable difference in the formation of the colloid was observed. Third, a further control study was performed where pure oxygen atmosphere was used in order to synthesize AQU/$n$$C_{60}$. Under the conditions otherwise identical to the ambient-atmosphere syntheses, this control experiment revealed no extraction-measurable formation of $n$$C_{60}$ aggregates after 168 h and a static light-scattering detector reading of only 1.40 V. This result is similar to the observed static light-scattering reading for P-I sample as summarized in Table 3.1.

Thus, instead of atmospheric O_2 acting as the oxygen source for the formation of $C_{60}O$ during the synthesis of AQU/$n$$C_{60}$, the trace amount of ozone naturally present in the atmosphere is more likely to be the source. As reported by Weisman, *et al.*, [12] and Heymann, *et al.*,[15] ozone is known to form the [6,6]-closed epoxide of C_{60} readily, both in solution and in the solid phase. In order to evaluate whether or not the trace level of ozone in the atmosphere is reasonable to be the source, the concentration of ozone required to form enough $C_{60}O$ to suspend the colloidal aggregates was determined. Indoor ozone concentrations vary by orders of magnitude with time-of-day, outdoor ozone level, outdoor/indoor air exchange rates, indoor sources of ozone, and many other factors.[19] The current OSHA recommended 8-hour limit for ozone concentrations is 100 ppb, however this limit is often exceeded during ozone advisories, such as were in effect during these experiments, and near certain electrical equipment. Assuming the 100 ppb as a reference value, in the 445 mL headspace of a 500 mL round-bottomed flask over a 100 mL sample (the experimental setup for this study) contains 1.2×10^{-9} mol O_3. In the 100 mL sample produced after a week under ambient conditions, the concentration of C_{60} in

the water was 0.41 ppm (as summarized in Table 1), or a total of 5.7×10^{-8} mol C_{60} in the 100 mL. Determination of $C_{60}O$ content by HPLC for sample P-I after a week stirring shows that 1.72% of $C_{60}O$ was available in the sample. To provide this amount of $C_{60}O$ in the suspensions, 9.8×10^{-10} mol ozone is required to convert the required amount of C_{60} to $C_{60}O$. This value is quite close to the estimated amount of ozone available (1.2×10^{-9} mol O_3). This estimate confirms that ambient levels of ozone are sufficiently high to account for the observed degree of fullerene derivatization, by keeping in my mind that the reaction occurs as proposed.

Based on this evidence, it is reasonable to propose an explanation that trace-levels of atmospheric ozone are responsible for the formation of $C_{60}O$, which then stabilizes AQU/*n*C_{60} in water. To confirm this hypothesis, another control study was performed. In a separate experiment, the trace levels of ozone present in the ambient atmosphere was removed from the system using the standard ozone scrubber potassium iodide.[20-22] Potassium iodide was dispersed from solution onto filter-paper and air-dried. The dried filter paper was then used to filter the air that was bubbled through and passed over the sample. Aliquots of this sample were obtained after 1, 24, 72, and 168 h of stirring. These samples showed no formation of *n*C_{60} aggregates after 168 h as measured by extraction and a static light-scattering detector reading of only 0.020 V. As can be seen from Table 3.1, this value shows that the dispersion of C_{60} in water was less favorable under the condition where atmospheric ozone was absent. The difference of the results obtained for the ambient ozone elimination using potassium iodide and nitrogen is due to the C_{60} starting material. It is important to note that the control experiment using potassium iodide was performed using a freshly-opened stock of C_{60}. In contrast to the fullerene

samples used elsewhere in this study that contained an initial 0.21% $C_{60}O$, the freshly-opened C_{60} stock was determined to have a $C_{60}O$ content below detectible limits. Therefore, not only does this control experiment demonstrate that ozone is the key atmospheric component responsible for the differences between the ambient- and inert-atmosphere samples, it also demonstrates that the trace amount of $C_{60}O$ present in the starting materials is responsible for the slight efficiency of colloid formation in inert-atmosphere samples such as P-I.

The explanation that ambient ozone is responsible for the formation of the $C_{60}O$ that is necessary to stabilize AQU/*n*C_{60} further explains the variability among labs in the ease of employing this method. Ambient ozone levels vary from day to day and from location to location. Similarly, the AQU/*n*C_{60} synthesis may take as little as a week or as long as a month to reach usable concentrations.

An alternate mechanism that might be proposed for the dependence of colloid formation on ozone is the autodecomposition of ozone in water to form hydroxyl radicals,[23] which can then attack fullerenes to form fullerols.[24] Such a mechanism would explain the observed ozone-dependence of the formation of AQU/*n*C_{60} and would be consistent with the known chemistries of ozone in aqueous systems and of hydroxyl radicals with fullerenes. In a recent study reported by Labille, *et al.*,[25] it is suggested that the mechanism of the formation of *n*C_{60} is due to the hydroxylation of the surface of C_{60} molecule when immersed in water. The primary evidence for the hydroxylation of the surface of C_{60} is from the infrared spectrum of the large, broad intense band near 1100 cm^{-1} attributed to C–O stretching (Figure 3.10).[26] Given the composition of the sample in

their study (a freeze-dried aqueous suspension of C_{60}), this C–O vibrations strongly suggest the presence of –OH groups in the nC_{60} structure.[27]

From the spectra reported in Labille's paper, a very clear albeit small peak below the 1100 cm^{-1} peak can be seen at approximately 750 – 850 cm^{-1}. While this peak was not explained by Labille, *et al.*, it is a characteristic transition of epoxides (symmetric and asymmetric stretches). This could possibly mean that the 1100 cm^{-1} peak have another source than the C–OH stretch of an alcohol as proposed by Labille, *et al*. C_{60} has a very strong Raman-active H_g vibrational mode at 1099 cm^{-1} that is IR inactive due to symmetry.[28] Breaking the symmetry through derivatization can make IR-inactive modes active. $C_{60}O$ has been reported to have broad peaks in this range, with the calculated vibrational modes that match this energy range.[29]

In response to Labille's report, another experiment was conducted to support the $C_{60}O$ formation during the synthesis of nC_{60}. In this experiment, a dried-down solution of C_{60} on a silicon wafer was prepared and then inverted on an attenuated total reflectance infrared spectrometer to get the IR spectrum of the C_{60} film. The film was then exposed to ozone under ambient conditions, and the spectrum was again taken as shown in Figure 3.10.

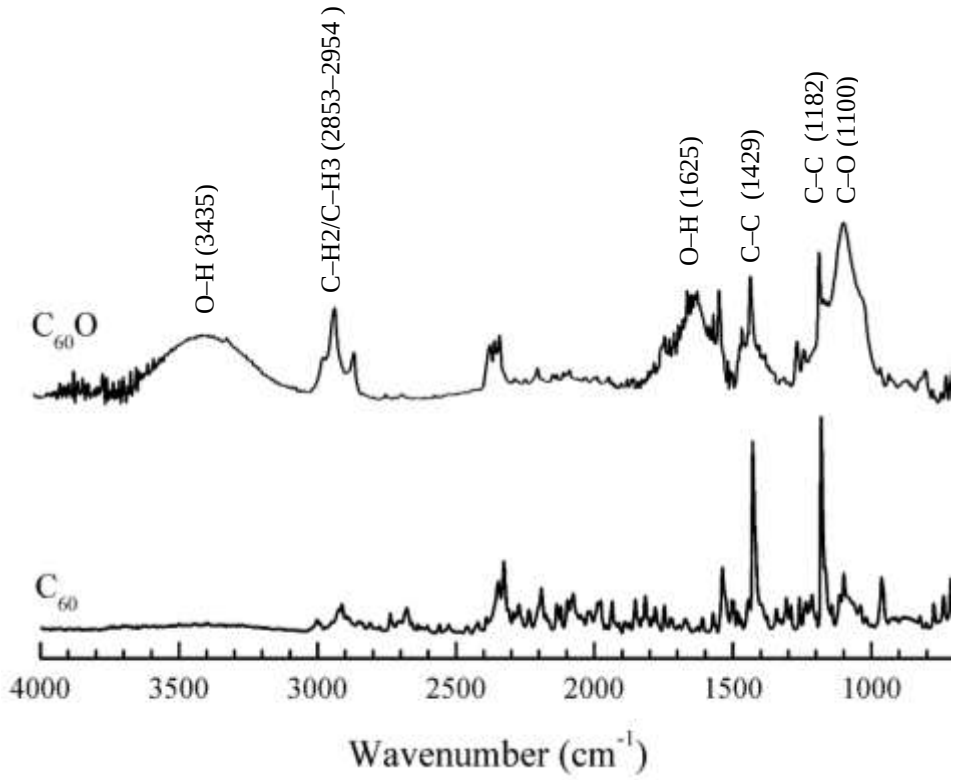

Figure 3.10. Infrared spectrum of C_{60} and ozonated C_{60}.

As can be seen in Figure 3.10, the 1100 cm^{-1} peak is present at very high intensity, quite similar to that shown for nC_{60} in the Labille paper. The broad water band at 3400 cm^{-1} is also clearly observed. It appears that once the system has been ozonated, it seems to absorb water out of the atmosphere with remarkable efficiency (the relative humidity on the day the experiment was performed was approximately 50%).

Given that the data from this study demonstrates a significant enrichment of the oxide and not the appearance of the fullerols, which have absorption spectra that are different from that of the oxide and should have retention times that are also different, it is apparent that the direct reaction of ozone with the fullerenes is a much more significant process in this system.

The effect of starting-material grain-size on dispersion kinetics

The rate of dispersion in these samples will undoubtedly depend to some degree on how finely-powdered the initial solids are. Since the starting materials used in this study have different grain-size, i.e the $C_{60}O$-enriched solid is finer than the pristine C_{60}, it is important to evaluate the possibility whether this grain-size effect might dominate the dispersion kinetics more than the effect of the C_{60}). In order to understand this effect, two new trials were conducted using deliberately reduced particle size of the starting pristine material.

In the first trial, the fullerene solids were ground following the procedure in Deguchi, *et al.*[30] in an agate mortar to obtained finely fullerene solids containing significant nanoparticulates. In the second trial, fullerene solids were dissolved in toluene followed by removal of the solvent by rotary evaporation, depositing a thin film of fullerenes on the inside surface of a round-bottomed flask. The second method was performed in a similar manner to the production of the $C_{60}O$-enriched starting material. Each of these samples was stirred in water under ambient conditions for an hour. Aliquots of each samples were taken and filtered similar to the other sample's aliquots as in the other experiments under controlled atmosphere.

The static light scattering detector voltages measured for each of these samples was in the lowest category shown in Table 2 (less than 0.09 volts), matching the static light scattering detector voltages observed for the corresponding P-A aliquot, and at least a factor of 25 lower than that of the corresponding O-A aliquot. Thus, while the grain size of the starting material may play some role in the dispersion kinetics, a smaller grain size

in our oxide-enriched samples cannot by-itself explain the differences observed between the P-A/P-I samples and the O-A/O-I samples.

The role of $C_{60}O$ in nC_{60} formed by other methods

An important factor to consider is that the 0.21% $C_{60}O$ present in the original C_{60} sample would likely have a different probability of partitioning into the colloidal phase from the solid phase than would the underivatized C_{60}. Since our percent yield for the entire colloid synthesis process is only 0.08% for sample P-A, most of the fullerene material, oxidized or not, is lost during the filtration step. Looked at another way, each original C_{60} molecule has a 0.08% chance of being incorporated into the final AQU/nC_{60} sample. It is reasonable to assume, however, that because of their greater hydrophilicity, the original $C_{60}O$ molecules will have a significantly greater chance of being incorporated into the final AQU/nC_{60} than do the pristine C_{60} molecules. Certainly the mobility of the individual molecules in the AQU/nC_{60} synthesis, a heterogeneous solid-liquid method, must be significantly limited. This lack of mobility means that the AQU/nC_{60} technique proceeds only extremely slowly in the absence of an alternate source of $C_{60}O$, as demonstrated by the extremely low, but non-zero, quantity of the colloid found in sample P-I. This model is further supported by a comparison of the colloid formation rates in samples O-A and O-I. Although both samples easily contain enough $C_{60}O$ to allow for the formation of the colloidal particles, the rate of formation is dramatically increased by the presence of trace atmospheric ozone. The significantly lower rate of oxide-molecule rearrangement to the colloidal particle surface in this heterogeneous solid-liquid system is

naturally slower than the addition of oxide molecules by reaction with atmospheric or dissolved ozone, which automatically occurs selectively at the surface.

Molecular mobility is not a problem, however, in other literature syntheses of *n*C_{60} because they start with the fullerenes dissolved in an organic solvent. When so dissolved, the C_{60} and $C_{60}O$ molecules are mobile enough to quickly and easily rearrange into a colloidal particle as the solubility of the fullerenes is dropped during synthesis, the hydrophilic portions of the $C_{60}O$ molecules partitioning to the surface. In preliminary experiments to test this hypothesis, we have synthesized *n*C_{60} by alternate literature methods and measured their $C_{60}O$ content by the methods described above. We have found in all cases that the resulting samples also contained significantly elevated amounts of $C_{60}O$. For example, despite that the original C_{60} contained 0.21% $C_{60}O$, the THF method[1,2] resulted in samples with 2.70% $C_{60}O$ and the toluene-sonication (SON) method[2,3] resulted in samples with 2.68% $C_{60}O$ (Figure 3.11).

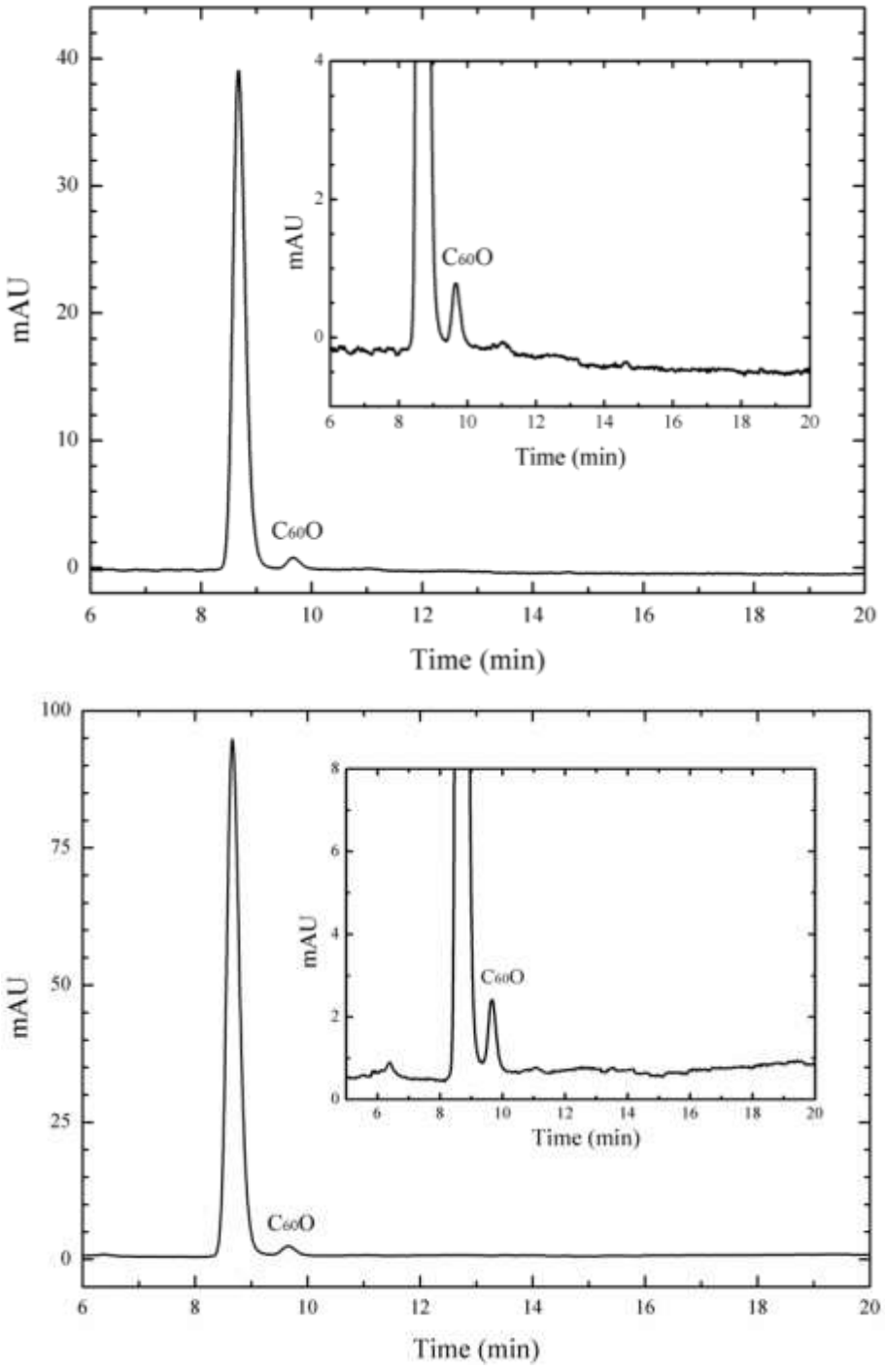

Figure 3.11. HPLC chromatogram at 336 nm of extracted *n*C_{60} samples prepared by THF (top) and SON (bottom) methods, showing the enhanced quantities of $C_{60}O$ relative to the 0.21% present in the original C_{60} sample.

Conclusions

Stabilization of C_{60} in water has been observed to be achieved due to the presence of its derivative, [6,6]-closed epoxide $C_{60}O$. The presence of ambient ozone is proposed to be the one responsible for the formation of [6,6]-closed epoxide $C_{60}O$. Even though the proposed mechanism of the formation of fullerols was reported to be the responsible for the stabilization of fullerene in water, the evidence in this study supports the possibility of oxide formation as the key component for the stabilization of fullerene in water.

References

1. Deguchi, S., Alargova, R. G. & Tsujii, K. Stable dispersions of fullerenes, C-60 and C-70, in water. Preparation and characterization. *Langmuir* **17**, 6013-6017, (2001).
2. Brant, J. A., Labille, J., Bottero, J. Y. & Wiesner, M. R. Characterizing the impact of preparation method on fullerene cluster structure and chemistry. *Langmuir* **22**, 3878-3885, (2006).
3. Andrievsky, G. V., Kosevich, M. V., Vovk, O. M., Shelkovsky, V. S. & Vashchenko, L. A. On the Production of an Aqueous Colloidal Solution of Fullerenes. *J Chem Soc Chem Comm*, 1281-1282, (1995).
4. Scrivens, W. A., Tour, J. M., Creek, K. E. & Pirisi, L. Synthesis of C-14-Labeled C-60, Its Suspension in Water, and Its Uptake by Human Keratinocytes. *J Am Chem Soc* **116**, 4517-4518, (1994).
5. Hilburn, M. E., Murdianti, B. S., Maples, R. D., Williams, J. S., Damron, J. T., Kuriyavar, S. I. & Ausman, K. D. Synthesizing aqueous fullerene colloidal suspensions by new solvent-exchange methods. *Colloids and Surfaces A: Physicochemical and Engineering Aspects* **401**, 48-53, (2012).
6. Labille, J., Brant, J., Villieras, F., Pelletier, M., Thill, A., Masion, A., Wiesner, M., Rose, J. & Bottero, J. Y. Affinity of C-60 fullerenes with water. *Fuller Nanotub Car N* **14**, 307-314, (2006).
7. Chibante, L. P. F. & Heymann, D. On the Geochemistry of Fullerenes - Stability of C-60 in Ambient Air and the Role of Ozone. *Geochim Cosmochim Ac* **57**, 1879-1881, (1993).

8. Cheng, X., Kan, A. T. & Tomson, M. B. Naphthalene Adsorption and Desorption from Aqueous C60 Fullerene. *J Chem Eng Data* **49**, 675 - 683, (2004).

9. Kazaoui, S., Ross, R. & Minami, N. In-Situ Photoconductivity Behavior of C-60 Thin-Films - Wavelength, Temperature, Oxygen Effect. *Solid State Commun* **90**, 623-628, (1994).

10. Bachilo, S. M., Benedetto, A. F. & Weisman, R. B. Triplet state dissociation of C-120, the dimer of C-60. *J Phys Chem B* **105**, 21a-22a, (2001).

11. Creegan, K. M., Robbins, J. L., Robbins, W. K., Millar, J. M., Sherwood, R. D., Tindall, P. J., Cox, D. M., Smith, A. B., Mccauley, J. P., Jones, D. R. & Gallagher, R. T. Synthesis and Characterization of (C60)O, the 1st Fullerene Epoxide. *J Am Chem Soc* **114**, 1103-1105, (1992).

12. Weisman, R. B., Heymann, D. & Bachilo, S. M. Synthesis and characterization of the "missing" oxide of C(60): [5,6]-open C(60)O. *J Am Chem Soc* **123**, 9720-9721, (2001).

13. Meier, M. S. & Kiegiel, J. Preparation and characterization of the fullerene diols 1,2-C-60(OH)(2), 1,2-C-70(OH)(2), and 5,6-C-70(OH)(2). *Organic Letters* **3**, 1717-1719, (2001).

14. Vileno, B., Marcoux, P. R., Lekka, M., Sienkiewicz, A., Feher, T. & Forro, L. Spectroscopic and photophysical properties of a highly derivatized C-60 fullerol. *Advanced Functional Materials* **16**, 120-128, (2006).

15. Heymann, D., Bachilo, S. M., Weisman, R. B., Cataldo, F., Fokkens, R. H., Nibbering, N. M. M., Vis, R. D. & Chibante, L. P. F. C60O3, a fullerene ozonide:

Synthesis end dissociation to C60O and O-2. *J Am Chem Soc* **122**, 11473-11479, (2000).

16. Heiney, P. A., Fischer, J. E., Mcghie, A. R., Romanow, W. J., Denenstein, A. M., Mccauley, J. P., Smith, A. B. & Cox, D. E. Orientational Ordering Transition in Solid C60. *Physical Review Letters* **66**, 2911-2914, (1991).
17. Arbogast, J. W., Darmanyan, A. P., Foote, C. S., Rubin, Y., Diederich, F. N., Alvarez, M. M., Anz, S. J. & Whetten, R. L. Photophysical Properties of C60. *J Phys Chem-Us* **95**, 11-12, (1991).
18. Palit, D. K., Sapre, A. V., Mittal, J. P. & Rao, C. N. R. Photophysical Properties of the Fullerenes, C-60 and C-70. *Chemical Physics Letters* **195**, 1-6, (1992).
19. Weschler, C. J. Ozone in indoor environments: Concentration and chemistry. *Indoor Air-International Journal of Indoor Air Quality and Climate* **10**, 269-288, (2000).
20. Calogirou, A., Larsen, B. R., Brussol, C., Duane, M. & Kotzias, D. Decomposition of terpenes by ozone during sampling on Tenax. *Analytical Chemistry* **68**, 1499-1506, (1996).
21. Fick, J., Pommer, L., Andersson, B. & Nilsson, C. Ozone removal in the sampling of parts per billion levels of terpenoid compounds: An evaluation of different scrubber materials. *Environmental Science & Technology* **35**, 1458-1462, (2001).
22. Grosjean, D., Williams, E. L. & Seinfeld, J. H. Atmospheric Oxidation of Selected Terpenes and Related Carbonyls - Gas-Phase Carbonyl Products. *Environmental Science & Technology* **26**, 1526-1533, (1992).

23. Yue, P. L. Modeling of Kinetics and Reactor for Water-Purification by Photooxidation. *Chemical Engineering Science* **48**, 1-11, (1993).

24. Guldi, D. M. & Asmus, K. D. Activity of water-soluble fullerenes towards (OH)-O-center dot-radicals and molecular oxygen. *Radiation Physics and Chemistry* **56**, 449-456, (1999).

25. Labille, J., Masion, A., Ziarelli, F., Rose, J., Brant, J., Villieras, F., Pelletier, M., Borschneck, D., Wiesner, M. R. & Bottero, J. Y. Hydration and dispersion of C60 in aqueous systems: the nature of water-fullerene interactions. *Langmuir* **25**, 11232-11235, (2009).

26. Lu, C. Y., Yao, S. D., Lin, W. Z., Wang, W. F., Lin, N. Y., Tong, Y. P. & Rong, T. W. Studies on the fullerol of C-60 in aqueous solution with laser photolysis and pulse radiolysis. *Radiat Phys Chem* **53**, 137-143, (1998).

27. Labille, J., Masion, A., Ziarelli, F., Rose, J., Brant, J., Villieras, F., Pelletier, M., Borschneck, D., Wiesner, M. R. & Bottero, J. Y. Hydration and Dispersion of C-60 in Aqueous Systems: The Nature of Water-Fullerene Interactions. *Langmuir* **25**, 11232-11235, (2009).

28. Neugebauer, J., Reiher, M., Kind, C. & Hess, B. A. Quantum chemical calculation of vibrational spectra of large molecules--Raman and IR spectra for Buckminsterfullerene. *J Comput Chem* **23**, 895-910, (2002).

29. Cardini, G., Bini, R., Salvi, P. R., Schettino, V., Klein, M. L., Strongin, R. M., Brard, L. & Smith, A. B. Infrared-Spectrum of 2 Fullerene Derivatives - C60o and C61h2. *J Phys Chem-Us* **98**, 9966-9971, (1994).

30. Deguchi, S., Mukai, S., Yamazaki, T., Tsudome, M. & Horikoshi, K. Nanoparticles of Fullerene C-60 from Engineering of Antiquity. *J Phys Chem C* **114**, 849-856, (2010).

CHAPTER IV

OXIDATIVE STUDY OF AQUEOUS C_{60} COLLOIDAL SUSPENSIONS

Introduction

Previous studies have demonstrated that fullerene in colloidal form can induce oxidative stress in living systems[1]. Different toxic responses due to fullerene exposure have been reported in bacteria, crustaceans, and fish with the lowest reported LC50 of 0.8 mg/l for *Daphnia magna* exposed for 48 h to C_{60} initially dissolved in tetrahydrofuran.[2-4] Previous studies by Sayes *et al* also have demonstrated that *n*C_{60} is highly cytotoxic to three human cell lines.[5,6] Its cytotoxicity appeared in that study to be associated with degree of derivatization. Additionally, these biological effects imply advantageous applications, such as *n*C_{60}'s potential utility as an effective antibacterial agent.[7-9]

Conflicting interpretations of these data have been presented in the literature. An oxidative-damage toxicity mechanism has been proposed by multiple researchers.[1,9] Other reports have suggested that some sample preparation methods can introduce organic solvent contaminants that are responsible for the observed oxidative damage.[10-12] Some of these studies monitor oxidation of sacrificial probe molecules, some trap

intermediate reactive oxygen species (ROS), and some monitor cell viability. No study to date, however, has successfully, systematically compared the nC$_{60}$ samples prepared by the synthesis techniques describe in the literature in terms of (1) oxidation of probe molecules, (2) production of various ROS, and (3) their ultimate effects on cells in culture.

The debate in the mechanism of cytotoxicity of aqueous fullerene aggregates is mostly centered on the potential behavior of nC$_{60}$ as an oxidant or as a generator of reactive oxygen species (ROS), and on the differences in samples produced by different techniques. The objective of this study is to explore the behavior of nC$_{60}$ prepared as oxidants. Detection of general oxidative behavior is performed using dihydrorhodamine 123 (DHR123), where it converts to a fluorescent molecule Rhodamine 123 upon introduction of an oxidant as described in the Figure 4.1 below.

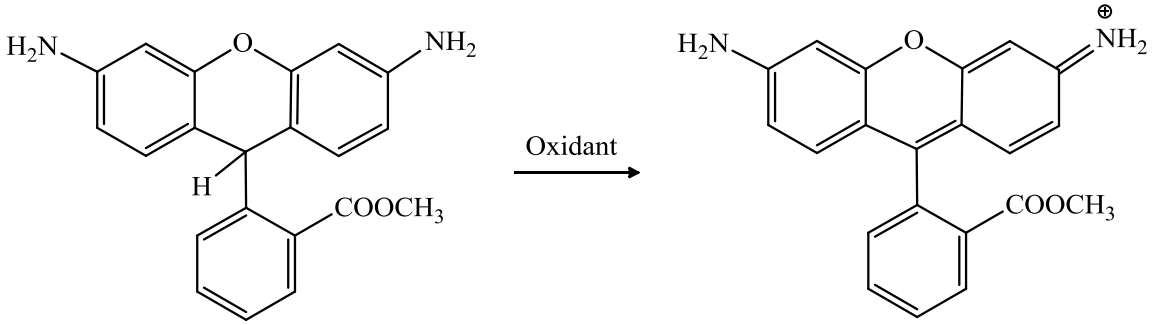

Figure 4.1. Oxidation of non-fluorescing molecule DHR123 to a fluorescing molecule Rhodamine 123.

Experimental

C$_{60}$ with 99.9% purity was purchased from MER Coorporation, Tucson, AZ. Ultrapure water used throughout the experiments was provided from Direct-Q 3 UV System

(Millipore, Billerica, MA) with resistivity greater than 18 MΩ·cm. Anhydrous Na_2SO_4 was purchased from Fisher Scientific, Fair Land, NJ. HPLC Grade toluene and tetrahydrofuran were purchased from Pharmco, Brookefield, CT. Dihydrorhodhamine 123 was purchased from Invitrogen™, Calrsbad, CA. Dimethyl sulfoxide was purchased from Sigma-Aldrich, St. Louis, MO.

Synthesis of *n*C_{60} samples

SON/*n*C_{60}. Approximately 100 mg of C_{60} solid was dissolved in 100 mL toluene and stirred overnight. Five mL of C_{60}/toluene solution was transferred to a 155 mm long test tube with inner and outer diameter of 29 mm and 32 mm, respectively. Twenty mL of ultrapure water was added and the test tube was immersed in a sonication bath and sonicated until all toluene evaporates from the mixture and the solution changed color from purple to brownish yellow. The temperature of the sonication bath was maintained below 40^{o}C. The suspension was then filtered through a 0.45-μm-MCE filter (Fisher Scientific, Denver, CO) to remove any undispersed material. Fullerene aggregate produced by this method (SON/*n*C_{60}) was characterized for particle size distribution by Malvern Instrument and for quantitative concentration determination by UV-visible spectroscopy.

THF/*n*C_{60}. Approximately 15 mg of C_{60} was dissolved in 500 mL tetrahydrofuran, stirred overnight and filtered through a glass filter to remove any undissolved material. Into a 500 mL round-bottom flask, 100 mL of nanopure water was added to 100 mL of C_{60}/THF solution with a flow rate of 1 L/min while the mixture was continuously stirred.

Upon addition of water, the solution immediately changed color from light magenta to yellow. Stirring was continued for another 30 minutes. Tetrahydrofuran was removed from the mixture by rotary evaporator at 35^{o}C and 200 mbar. When most of the tetrahydrofuran was removed, pressure was gradually reduced to reach 60 mbar. The suspension was diluted 3 times using 20 mL nanopure water each, and the added water was removed by rotary evaporator. After removal of additional water , the suspension was filtered through a 0.45-μm-MCE filter (Fisher Scientific, Denver, CO) to remove any undispersed material. Fullerene aggregate produced by this method (THF/*n*C_{60}) was characterized for particle size distribution performed on a Malvern High Performance Particle Sizer, model HPP5001 by Malvern Instruments and for quantitative concentration determination by UV-visible spectroscopy.

DHR123 solution

2.5 mg of DHR123 was dissolved in 100 mL dimethyl sulfoxide (DMSO). The solution was sealed under nitrogen gas and stored in the dark at low temperature if not used, to minimize the oxidation of DHR123 to Rhodamine 123. Prior using, the DHR123/DMSO solution was thawed at ambient temperature in the dark.

Oxidation measurement

Fluorescence intensity of Rhodamine 123 was measured using Fluorolog®-3 spectrofluorometer (HORIBA Scientific). Experiments were performed under inert and ambient conditions. Three mL of ultrapure water and a small stir bar was transferred to a cuvette, where 50 μL of DHR123/DMSO solution was then added. For inert condition

experiment, ultrapure water in the cuvette was initially purged with nitrogen gas and capped with a screw cap equipped with septum seal before addition of DHR123/DMSO. Fullerene colloidal samples for inert condition experiment were also sealed and purged with nitrogen gas for 30 minutes. The cuvette was fixed into a fluorometer and data was collected for the first 300*s* with 1*s* interval while the mixture was continuously stirred. Two hundred microliters of *n*C_{60} sample was added quickly using a micro syringe and data was collected for another 1500*s* with 1*s* interval. The wavelengths used for excitation and emission were 485 and 530 nm, respectively. Five different concentrations of THF/*n*C_{60} (0.14, 0.24, 0.46, 0.69, and 0.90 mg/L) and SON/*n*C_{60} (0.26, 0.51, 1.02, 2.01, and 3.89 mg/L) were used.

Result and Discussions

The concentration of C_{60} aggregates was determined using extraction method as described in Chapter 3. Stock solution of THF/*n*C_{60} has a concentration of 14.6 mg/L with average diameter of the particles of 84.7 nm, while SON/*n*C_{60} has a concentration of 63.2 mg/L with average diameter of 111.8 nm.

General oxidation study with *n*C_{60} aggregates was performed using THF/*n*C_{60} and SON/*n*C_{60} methods due to their ease in preparation to obtain high concentration of *n*C_{60} dispersed in water. Introduction of THF/*n*C_{60} or SON/*n*C_{60} to the DHR 123 system increases the fluorescence intensity of the molecular probe as observed by fluorometer as seen in Figure 4.2. With increasing the concentrations of THF/*n*C_{60} or SON/*n*C_{60}, an

increase of fluorescence intensity was also observed, indicating that the oxidation reaction of DHR123 to rhodamine123 occurs faster.

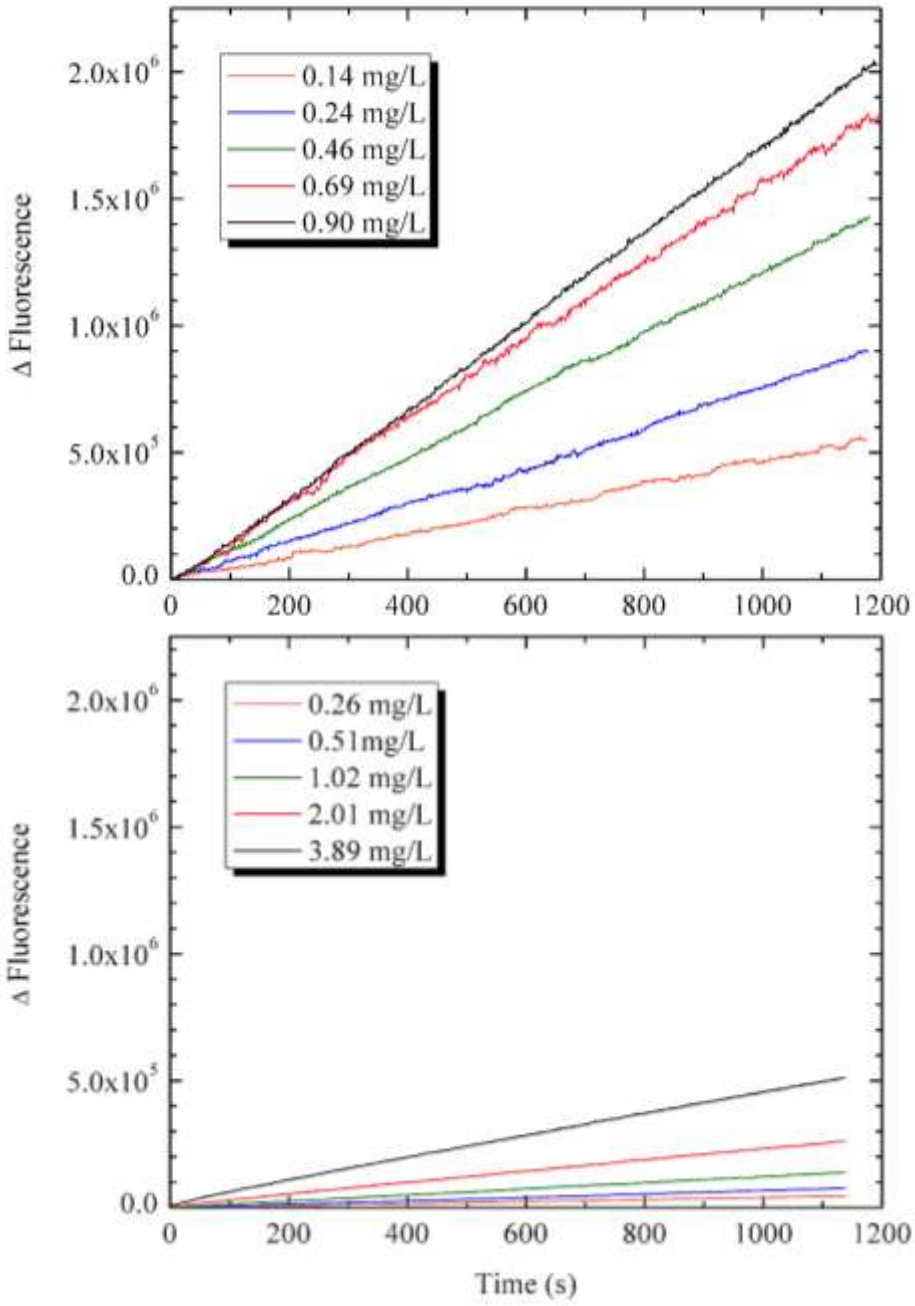

Figure 4.2. Fluorescence spectra of rhodamine123 after introducing THF/nC$_{60}$ (top) and SON/nC$_{60}$ (bottom) to DHR123 system.

In the study using THF/*n*C_{60}, more DHR123 was converted to rhodamine123 as compared to the study using SON/*n*$C_{60.}$ Using the highest concentration of THF/*n*C_{60} (0.90 mg/L) introduced to the system, higher concentration of rhodamine123 was observed to be approximately 4 times higher than introducing the highest concentration of SON/*n*C_{60} (3.89 mg/L) to the system. This result indicates that THF/*n*C_{60} acts more as an oxidant as compared to SON/*n*C_{60} aggregates. The significant difference in the ability of THF/*n*C_{60} and SON/*n*C_{60} aggregates to convert DHR123 to rhodamine123 is probably due to the presence of other compounds from tetrahydrofuran oxidation products (*e.g.* γ-butyrolactone) during the synthesis of THF/*n*C_{60} as reported by Henry, *et al.* and Sphon, *et al*.[13,14] Even though other oxidation products from tetrahydrofuran may contribute to the oxidation of DHR123 observed, it should be noted that in the SON/*n*C_{60} which does not contain oxidation products such as γ-butyrolactone, oxidation of DHR123 was also observed.

Due to the concern that ambient atmosphere may contribute to the observed oxidation of DHR123, the oxidation study of *n*C_{60} aggregate was also conducted at inert atmosphere. Eliminating ambient air from the system significantly reduced the conversion of DHR123 to rhodamine123 when THF/*n*C_{60} was introduced to the system (Figure 4.3), while only a small difference of the oxidation behavior was observed when using SON/*n*C_{60} (Figure 4.4).

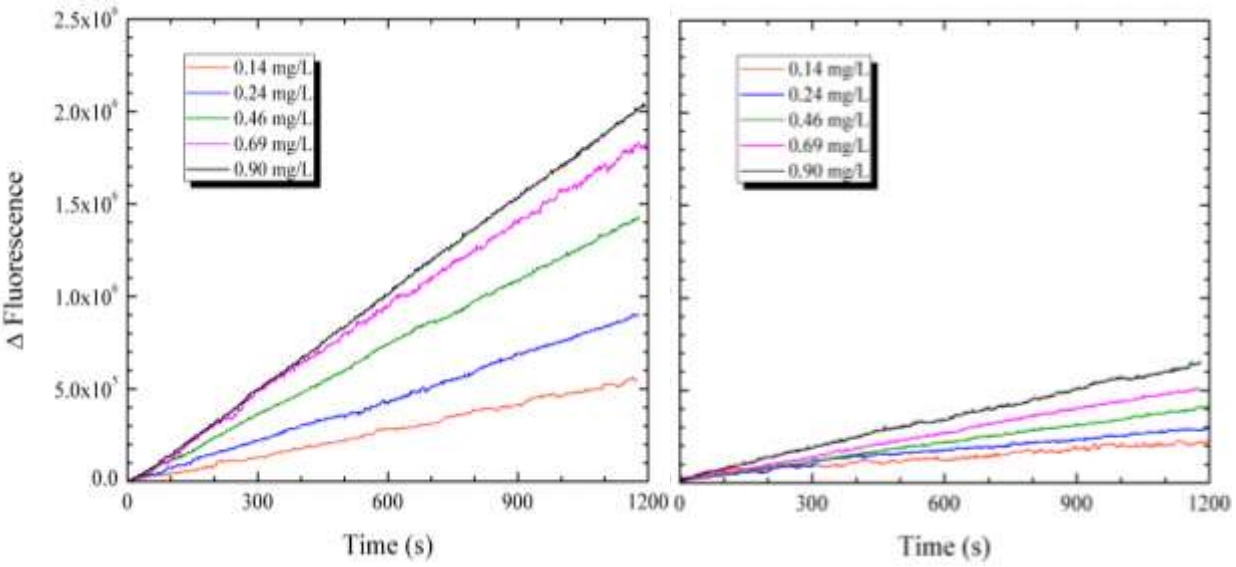

Figure 4.3. Oxidation of DHR123 to rhodamine123 using THF/*n*C_{60} at ambient (left) and inert (right) atmosphere

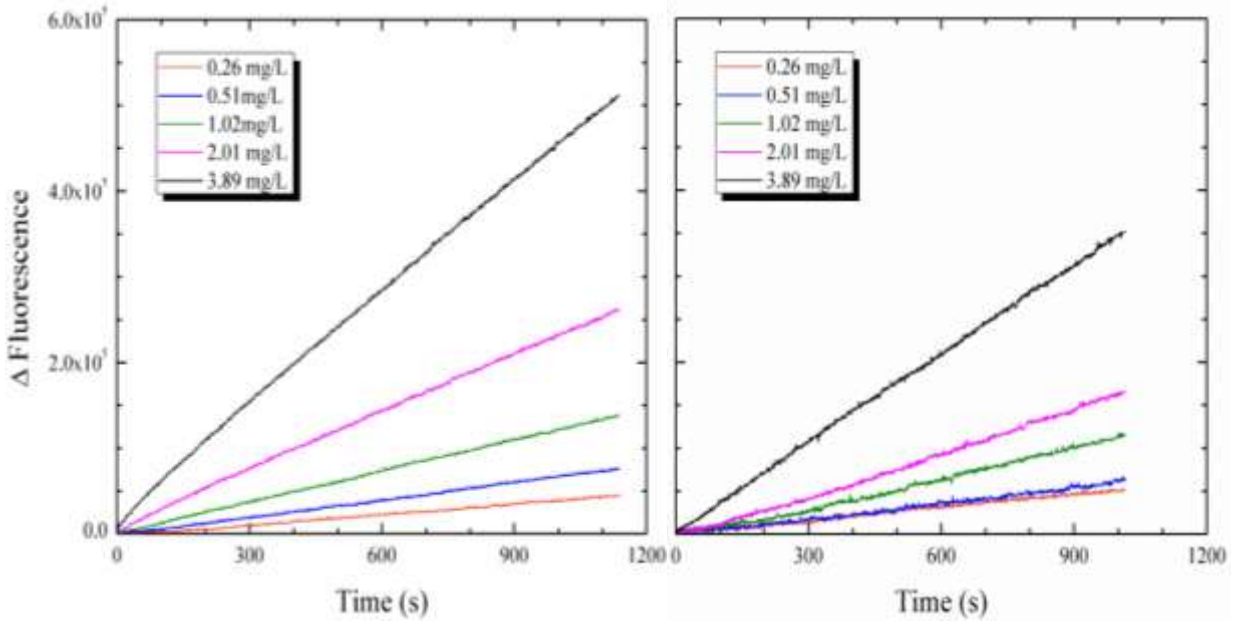

Figure 4.4 Oxidation of DHR123 to rhodamine123 using SON/*n*C_{60} at ambient (left) and inert (right) atmosphere

Considering that in the synthesis of THF/*n*C_{60} there may still be some residual tetrahydrofuran,[13,15] and that with the presence of oxygen tetrahydrofuran can be oxidized into 2-hydroxytetrahydrofuran and γ-butyrolactone,[13] the observed significant difference of the rhodamine123 production between the ambient and inert atmosphere of THF/*n*C_{60} may be due to the oxidation of DHR123 from residual tetrahydrofuran in the *n*C_{60} suspensions, including the hydroperoxide degradation products. In the THF/*n*C_{60} sample, trace amount of tetrahydrofuran may still be present. Since tetrahydrofuran reacts readily with oxygen to form hydroperoxide that can act as an oxidant, eliminating the supply of oxygen in a closed system such as in the preparation of ambient atmosphere sample in this study, limits the formation of peroxides. Because the peroxides are unstable, and the source of atmospheric oxygen is limited, the decomposition of tetrahydrofuran peroxides may occur before the oxidation study starts, giving significant decrease of oxidative behavior reaction of DHR123 with inert atmosphere samples. In SON/*n*C_{60}, similar behavior was not observed because of the absence of easily oxidized organic solvent. This preliminary hypothesis needs to be confirmed by further experimentation.

The linearity of the plot of the concentration of rhodamine123 vs. time suggests that the oxidation reaction obeys zeroth order kinetics. However, these preliminary results, while they clearly indicate that oxidation still occurs in *n*C_{60} samples even without the presence of THF degradation products, suffer from problems of quantitative reproducibility, satisfactory mixing, and the lack of a good model to account for the observed zeroth-order behavior.

Conclusions

Eventhough the presence of degradation products from tetrahydrofuran has been proposed to cause toxicity of *n*C_{60}, it has been observed from this study that preparation of *n*C_{60} with or without tetrahydrofuran induced significant oxidation of the probe molecule DHR123. The oxidizing behavior of *n*C_{60} requires further investigation, especially for the oxidative behavior of key fullerene derivatives, such as the oxides that are found to play an important role in the formation of aqu/*n*C_{60} samples.

References

1. Oberdorster, E. Manufactured nanomaterials (fullerenes, C_{60}) induce oxidative stress in the brain of juvenile largemouth bass. *Environmental Health Perspective* **112**, 1058-1062, (2004).
2. Fortner, J. D., Lyon, D. Y., Sayes, C. M., Boyd, A. M., Falkner, J. C., Hotze, E. M., Alemany, L. B., Tao, Y. J., Guo, W., Ausman, K. D., Colvin, V. L. & Hughes, J. B. C60 in water: nanocrystal formation and microbial response. *Environ Sci Technol* **39**, 4307-4316, (2005).
3. Oberdorster, E., Zhu, S. Q., Blickley, T. M., McClellan-Green, P. & Haasch, M. L. Ecotoxicology of carbon-based engineered nanoparticles: Effects of fullerene (C-60) on aquatic organisms. *Carbon* **44**, 1112-1120, (2006).
4. Zhu, S. Q., Oberdorster, E. & Haasch, M. L. Toxicity of an engineered nanoparticle (fullerene, C-60) in two aquatic species, Daphnia and fathead minnow. *Mar Environ Res* **62**, S5-S9, (2006).
5. Sayes, C. M., Fortner, J. D., Guo, W., Lyon, D., Boyd, A. M., Ausman, K. D., Tao, Y. J., Sitharaman, B., Wilson, L. J., Hughes, J. B., West, J. L. & Colvin, V. L. The differential cytotoxicity of water-soluble fullerenes. *Nano Lett* **4**, 1881-1887, (2004).
6. Sayes, C. M., Gobin, A. M., Ausman, K. D., Mendez, J., West, J. L. & Colvin, V. L. Nano-C-60 cytotoxicity is due to lipid peroxidation. *Biomaterials* **26**, 7587-7595, (2005).
7. Fortner, J. D., Lyon, D. Y., Sayes, C. M., Boyd, A. M., Falkner, J. C., Hotze, E. M., Alemany, L. B., Tao, Y. J., Guo, W., Ausman, K. D., Colvin, V. L. &

Hughes, J. B. C_{60} in water: nanocrystal formation and microbial response. *Environ. Sci. Technol.* **39**, 4307-4316, (2005).

8. Sayes, C. M., Fortner, J. D., Guo, W., Lyon, D. Y., Boyd, A. M., Tao, Y. J., Sitharaman, B., Wilson, L. J., Hughes, J. B., West, J. L. & Colvin, V. L. The differential cytotoxicity of water-soluble fullerenes. *Nano Letters* **4**, 1881-1887, (2004).

9. Sayes, C. M., Gobin, A. M., Ausman, K. D., Mendez, J., West, J. L. & Colvin, V. L. Nano-C_{60} cytotoxicity is due to lipid peroxidation. *Biomaterial* **26**, 7587-7595, (2005).

10. Andrievsky, G., Klochkov, V. & Derevyanchenko, L. Is the C_{60} fullerene molecule toxic? *Fullerenes, Nanotubes and Carbon Nanostructures* **13**, 363-376, (2005).

11. Gharbi, N., Pressac, M., Hadchouel, M., Szwarc, H., Wilson, S. R. & Moussa, F. [60]fullerene is a powerful antioxidant in vivo with no acute or subacute toxicity. *Nano Lett* **5**, 2578-2585, (2005).

12. Isakovic, A., Markovic, Z., Nikolic, N., Todorovic-Markovic, B., Vranjes-Djuric, S., Harhaji, L., Raicevi, N., Romcevic, N., Vasiljevic-Radovic, D., Dramicanin, M. & Trajkovic, V. Inactivation of nanocrystalline C-60 cytotoxicity by gamma-irradiation. *Biomaterials* **27**, 5049-5058, (2006).

13. Spohn, P., Hirsch, C., Hasler, F., Bruinink, A., Krug, H. F. & Wick, P. C-60 fullerene: A powerful antioxidant or a damaging agent? The importance of an in-depth material characterization prior to toxicity assays. *Environ Pollut* **157**, 1134-1139, (2009).

14. Henry, T. B., Menn, F. M., Fleming, J. T., Wilgus, J., Compton, R. N. & Sayler, G. S. Attributing effects of aqueous C60 nano-aggregates to tetrahydrofuran decomposition products in larval zebrafish by assessment of gene expression. *Environ Health Perspect* **115**, 1059-1065, (2007).

15. Andrievsky, G., Klochkov, V. & Derevyanchenko, L. Is the C-60 fullerene molecule toxic?! *Fuller Nanotub Car N* **13**, 363-376, (2005).

CHAPTER V

CONCLUSIONS AND FUTURE WORK

Stable C_{60} aqueous suspensions are complex systems that are poorly understood and need further study in order to understand their behavior. Through different synthesis methods, it has been reported that the obtained suspensions have varied properties in terms of particle size, concentration, surface charge, surface chemistry, contaminant concentrations, synthesis reproducibility, and toxicity.[1-8]

Stabilization of C_{60} in water has been reported due to the surface hydroxylation of the initially hydrophobic C_{60} molecule.[9] In this study, however, evidence of the formation of the [6,6]-closed epoxide $C_{60}O$ on the surface of C_{60} molecule was observed as a key component to cause the stabilization of the colloidal particles in water. The formation of [6,6]-closed epoxide $C_{60}O$ was due to the small fraction of ambient ozone presence in the atmosphere.

Giving into account that the auto decomposition of ozone in water forms hydroxyl radicals[10] which can then attack fullerene to form fullerols[11] and the proposed mechanism of the formation of nC_{60} is due to the hydroxylation of the surface of C_{60} when immersed in water,[9] a future direction from this study is to further investigate whether hydroxylation might play minor role in the stabilization of the colloidal particles in water.

In the study of nC$_{60}$ oxidative behavior, there is a significant difference in the oxidation of DHR123 to rhodamine123 between THF/nC$_{60}$ and SON/nC$_{60}$. The difference observed is due to the presence of auto decomposition products from tetrahydrofuran. In the preliminary data on nC$_{60}$ oxidative behavior, it is observed that nC$_{60}$ colloidal aggregates prepared without controversial solvent tetrahydrofuran also induced significant oxidation of the probe molecule DHR123. From this preliminary data, and given that C$_{60}$O epoxide acts as a key component for the stabilization of C$_{60}$ colloidal suspensions in water, it is important to further investigate the oxidation mechanism of nC$_{60}$ and the possibility of the C$_{60}$O to induce oxidation. Since the use of DHR123 in DMSO may give misleading observation, the use of DHR123 salts is suggested in this study, to avoid organic solvents to be present in the system.

References

1. Chae, S. R., Badireddy, A. R., Farner Budarz, J., Lin, S., Xiao, Y., Therezien, M. & Wiesner, M. R. Heterogeneities in fullerene nanoparticle aggregates affecting reactivity, bioactivity, and transport. *Acs Nano* **4**, 5011-5018, (2010).
2. Andrievsky, G. V., Kosevich, M. V., Vovk, O. M., Shelkovsky, V. S. & Vashchenko, L. A. On the Production of an Aqueous Colloidal Solution of Fullerenes. *J Chem Soc Chem Comm*, 1281-1282, (1995).
3. Brant, J. A., Labille, J., Bottero, J. Y. & Wiesner, M. R. Characterizing the impact of preparation method on fullerene cluster structure and chemistry. *Langmuir* **22**, 3878-3885, (2006).
4. Deguchi, S., Alargova, R. G. & Tsujii, K. Stable dispersions of fullerenes, C-60 and C-70, in water. Preparation and characterization. *Langmuir* **17**, 6013-6017, (2001).
5. Hilburn, M. E., Murdianti, B. S., Maples, R. D., Williams, J. S., Damron, J. T., Kuriyavar, S. I. & Ausman, K. D. Synthesizing aqueous fullerene colloidal suspensions by new solvent-exchange methods. *Colloids and Surfaces A: Physicochemical and Engineering Aspects* **401**, 48-53, (2012).
6. Labille, J., Brant, J., Villieras, F., Pelletier, M., Thill, A., Masion, A., Wiesner, M., Rose, J. & Bottero, J. Y. Affinity of C-60 fullerenes with water. *Fuller Nanotub Car N* **14**, 307-314, (2006).
7. Scrivens, W. A., Tour, J. M., Creek, K. E. & Pirisi, L. Synthesis of C-14-Labeled C-60, Its Suspension in Water, and Its Uptake by Human Keratinocytes. *J Am*

Chem Soc **116**, 4517-4518, (1994).

8. Song, M., Yuan, S., Yin, J., Wang, X., Meng, Z., Wang, H. & Jiang, G. Size-dependent toxicity of nano-C60 aggregates: more sensitive indication by apoptosis-related Bax translocation in cultured human cells. *Environ Sci Technol* **46**, 3457-3464, (2012).
9. Labille, J., Masion, A., Ziarelli, F., Rose, J., Brant, J., Villieras, F., Pelletier, M., Borschneck, D., Wiesner, M. R. & Bottero, J. Y. Hydration and Dispersion of C-60 in Aqueous Systems: The Nature of Water-Fullerene Interactions. *Langmuir* **25**, 11232-11235, (2009).
10. Yue, P. L. Modeling of Kinetics and Reactor for Water-Purification by Photooxidation. *Chem Eng Sci* **48**, 1-11, (1993).
11. Guldi, D. M. & Asmus, K. D. Activity of water-soluble fullerenes towards (OH)-O-center dot-radicals and molecular oxygen. *Radiat Phys Chem* **56**, 449-456, (1999).

VITA

Befrika Saparia Murdianti

Candidate for the Degree of

Doctor of Philosophy

Thesis: STABILITY OF NANO-ENGINEERED C_{60} COLLOIDAL SUSPENSIONS IN WATER AND ITS OXIDATIVE BEHAVIOR

Major Field: Physical Chemistry

Biographical:

Education:

Completed the requirements for the Doctor of Philosophy in Chemistry at Oklahoma State University, Stillwater, Oklahoma in July, 2012.

Completed the requirements for the Master of Science in Chemistry at The University of Tulsa, Tulsa, OK in 2007.

Completed the requirements for the Bachelor of Science in Chemistry at Institut Teknologi Bandung, Bandung-West Java, Indonesia in 2000.

Experience: Laboratory Assistant, Department of Chemistry, Institut Teknologi Bandung (July 1997–October 2000). Business Development, Pharos Pharmaceutical, Indonesia (January 2001–April 2001). Laboratory Supervisor, Charoen Pokphand Indonesia (June 2001–August 2002). Teaching Assistant, Department of Chemistry and Biochemistry, The University of Tulsa (January 2005–December 2006). Research Assistant, Center for Applied Bio-Geosciences, The University of Tulsa (January 2007–May 2007). Teaching Assistant, Department of Chemistry, Oklahoma State University (August 2007–May 2012).

Professional Memberships: American Chemical Society, Iota Sigma Pi National Honor Society of Women in Chemistry, Graduate and Professional Student Government Association

Name: Befrika S. Murdianti Date of Degree: July, 2012

Institution: Oklahoma State University Location: Stillwater, Oklahoma

Title of Study: STABILITY OF NANO-ENGINEERED C_{60} COLLOIDAL SUSPENSIONS IN WATER AND ITS OXIDATIVE BEHAVIOR

Pages in Study: 92 Candidate for the Degree of Doctor of Philosophy

Major Field: Physical Chemistry

Scope and Method of Study:

Following the discovery of C_{60} in 1985, the compound has attracted much research due to its unique properties and wide array of potential applications from drug delivery to energy conversion. Multi-ton production of this compound began in 2003, and thus concerns of the fate of C_{60} in the environment began to be taken seriously. Although C_{60} has low solubility in water, it can form a stable aqueous colloidal suspension (termed nC_{60}) through several methods, such as solvent exchange from organic solvents or long-term vigorous stirring in water. Literature reports have been seemingly contradictory about the stability, form, and environmental and health effects of this aqueous colloidal form. This study discuss the role of the [6,6]-closed epoxide derivative of C_{60} ($C_{60}O$) in the formation and stabilization of the colloidal aggregates. Additionally, the oxidative behavior of nC_{60} as evaluated using the probe molecule dihydrorhodamine-123 (DHR 123) is also discussed.

Findings and Conclusions:

Stabilization of C_{60} colloidal particle in water is due to the formation of [6,6]-closed epoxide of C_{60}. This derivative is present in small quantities due to the reaction with air. In the aqu/nC_{60} method, or the vigorous stirring of C_{60} solid in water, the presence of trace level of ozone in the ambient air is required for the formation of nC_{60} to produce sufficient $C_{60}O$ formation on the surface of nC_{60} particle to allow stable dispersion in water. Elimination of ambient air during the synthesis of aqu/nC_{60} significantly retards the formation of nC_{60} due to the inability to produce $C_{60}O$. Eventhough other mechanism of stabilization of C_{60} in water such as hydroxylation of C_{60} has been proposed, this study strongly suggest that $C_{60}O$ plays an important role in stabilizing C_{60} colloidal suspensions in water. In the study of nC_{60} oxidative behavior using nC_{60} prepared using tetrahydrofuran and toluene, it has been shown that both preparation methods induce significant oxidation of the molecular probe DHR123. The formation of $C_{60}O$ during nC_{60} synthesis may give contribution to the observed oxidation.

ADVISER'S APPROVAL: Dr. Kevin Ausman